CEM KAAN ŞEN
A COMPARATIVE STUDY ON THE PERFORMANCE OF PLA AND PET ACOUSTIC PERFORATED PANELS
Bilkent University 2025

A COMPARATIVE STUDY ON THE PERFORMANCE OF PLA AND PET ACOUSTIC PERFORATED PANELS

A Master’s Thesis

by
CEM KAAN ŞEN

Department of
Interior Architecture and Environmental Design
İhsan Doğramacı Bilkent University
Ankara
August 2025

To Oya…

A COMPARATIVE STUDY ON THE PERFORMANCE OF PLA AND PET ACOUSTIC PERFORATED PANELS

The Graduate School of Economics and Social Sciences
of
İhsan Doğramacı Bilkent University

by

CEM KAAN ŞEN

In Partial Fulfillment of the Requirements for the Degree of
MASTER OF FINE ARTS IN INTERIOR ARCHITECTURE AND ENVIRONMENTAL DESIGN

THE DEPARTMENT OF
INTERIOR ARCHITECTURE AND ENVIRONMENTAL DESIGN
İHSAN DOĞRAMACI BİLKENT UNIVERSITY
ANKARA

August 2025

A COMPARATIVE STUDY ON THE PERFORMANCE OF PLA AND PET ACOUSTIC PERFORATED PANELS
By Cem Kaan Şen

I certify that I have read this thesis and have found that it is fully adequate, in scope and in quality, as a thesis for the degree of Master of Fine Arts in Interior Architecture and Environmental Design.

Semiha Yılmazer
Advisor

I certify that I have read this thesis and have found that it is fully adequate, in scope and in quality, as a thesis for the degree of Master of Fine Arts in Interior Architecture and Environmental Design.

Arzu Gönenç Sorguç
Examining Committee Member

I certify that I have read this thesis and have found that it is fully adequate, in scope and in quality, as a thesis for the degree of Master of Fine Arts in Interior Architecture and Environmental Design.

Nuri Cihan Kayaçetin
Examining Committee Member

Approval of the Graduate School of Economics and Social Sciences

----
Refet S. Gürkaynak
Director

ABSTRACT

A COMPARATIVE STUDY ON THE PERFORMANCE OF PLA AND PET ACOUSTIC PERFORATED PANELS

Şen, Cem Kaan

MFA., Interior Architecture and Environmental Design

Supervisor: Assist. Prof. Dr. Semiha Yılmazer

August 2025

The growing demand for high-performance low-frequency sound absorbers in architectural acoustics requires sustainable alternatives to conventional sound-absorbing materials. The present study investigates the acoustic performance of Micro-Perforated Panels (MPP) made from organic and inorganic 3D printed thermoplastics utilizing Fused Deposition Modelling (FDM). Following this gap in the literature, the research compares biodegradable polylactic acid (PLA) based (MPP1) and recycled polyethylene terephthalate (PET) based (MPP2) MPPs as sustainable alternatives to classroom settings. To compare with conventional materials from previous literature, inhomogeneous MPP configurations were manufactured for each material type. Their sound absorption coefficients (α) were tested with ISO 10534-2:2023 using an impedance tube and were evaluated in a classroom simulation based on ODEON Room Acoustics Software Version 18.0 to assess their impact on reducing Reverberation Time (RT30) and increasing Speech Transmission Index (STI) scores. The results indicated that both materials demonstrated similar α values in mid to higher frequencies, while MPP2 performed better in lower frequencies. Subsequently, the measured and simulated measurements of RT30 in the classroom in Bilkent University showed that the room is acoustically undertreated. The introduced materials in the simulation indicated that treatment with MPP1 reduced RT30 from 1.25s average to 1s, and treatment with MPP2 reduced RT30 to 0.85s. The STI results increased from 0.51 to 0.6, improving from “fair” to “good” speech intelligibility scores. Overall, the findings highlighted the potential of recycled and biodegradable MPPs to serve as a viable alternative to sustainable sound-absorbing materials in university classroom settings. For future studies, recycled sound absorbers could replace conventional sound absorbers in architectural acoustics.

Keywords: Classroom Acoustics, Micro-Perforated Panels (MPP), Reverberation Time (RT), Sound Absorption Coefficient, Speech Transmission Index (STI), Sustainable Materials

ÖZET

PLA VE PET AKUSTİK DELİKLİ PANELLERİN PERFORMANSI ÜZERİNE KARŞILAŞTIRMALI BİR ÇALIŞMA

Şen, Cem Kaan
Yüksek Lisans, İç Mimarlık ve Çevre Tasarımı
Tez Danışmanı: Dr. Öğr. Üyesi Semiha Yılmazer

Ağustos 2025

Mimari akustik alanında yüksek performanslı, düşük frekanslı ses yutuculara yönelik artan talep, geleneksel ses yutucu malzemelere sürdürülebilir alternatiflerin geliştirilmesini gerekli kılmaktadır. Bu çalışma, Kaynaşık Yığma Modelleme (Fused Deposition Modelling_FDM) tekniğiyle 3B yazıcıda üretilen organik ve inorganik Mikro Delikli Panellerin (Micro-Perforated Panel_MPP) akustik performansını incelemektedir. Literatürdeki bu boşluğu doldurmak adına, araştırma, biyolojik olarak parçalanabilen polilaktik asit (PLA) bazlı (MPP1) ve geri dönüştürülmüş polietilen tereftalat (PET) bazlı (MPP2) MPP'leri bir sınıf ortamında sürdürülebilir bir alternatif olarak karşılaştırmaktadır. Önceki çalışmalardaki geleneksel malzemelerle karşılaştırma yapılabilmesi amacıyla, her malzeme türü için paralel olarak düzenlenmiş heterojen MPP konfigürasyonları üretilmiştir. Ses yutma katsayıları (α), ISO 10534-2:2023 standardına uygun olarak empedans tüpüyle ölçülmüş, Reverberasyon Süresi (Reverberation Time_RT30) ve Konuşma İletim İndeksi (Speech Transmission Index_STI) üzerindeki etkileri ise ODEON Akustik Simülasyon Yazılımı Versiyon 18.0 ile sınıf ortamında incelenmiştir. Sonuçlar, her iki malzemenin de orta ve yüksek frekanslarda benzer α değerleri sergilediğini, ancak MPP2'nin düşük frekanslarda daha iyi performans gösterdiğini ortaya koymuştur. Bilkent Üniversitesi'ndeki sınıf ortamında yapılan ölçümler ve simülasyonlar, mevcut akustik düzenlemenin yetersiz olduğunu göstermiştir. Simülasyonda kullanılan malzemelerden MPP1, ortalama RT30 değerini 1,25 saniyeden 1 saniyeye indirirken, MPP2 bu süreyi ortalama 0,85 saniyeye kadar düşürmüştür. STI sonuçları ise 0.51'den 0.6'ya yükselerek konuşma anlaşılırlığını (Speech Intelligibility) "orta" seviyeden “iyi” seviyeye taşımıştır. Genel olarak, sonuçlar geri dönüştürülmüş ve biyoçözünür MPP’lerin üniversite sınıfı gibi iç mekânlarda sürdürülebilir ses yutucu malzemelere geçişte uygulanabilir alternatifler sunduğunu ortaya koymaktadır. Gelecekte yapılacak çalışmalar için, geri dönüştürülmüş ses yutucuların geleneksel malzemelerin yerini alma potansiyeli değerlendirilmesi önerilmektedir.

Anahtar Kelimeler: Konuşma İletim İndeksi (STI), Mikro Delikli Paneller (MPP), Reverberasyon Süresi (RT), Ses Yutma Katsayısı, Sınıf Akustiği, Sürdürülebilir Malzemeler

ACKNOWLEDGEMENTS

It has been a long and challenging academic journey, which I was not sure about beginning. First and foremost, I am very grateful to have such a wonderful advisor, Assist. Prof. Semiha Yılmazer. Her guidance and support, even in the darkest times, showed that writing a thesis is nothing to be afraid of.

I would like to express my gratitude to the members of the examining committee, Prof. Dr. Arzu Gönenç Sorguç and Assist. Prof. Nuri Cihan Kayaçetin for their valuable feedback and contributions to the future of this work.

I am more than grateful to my family, especially my parents, who never wavered in their support for me with their unconditional love. My warmest thanks go to my sister for always encouraging me to thrive and motivating me through all the academic struggles.

My sincerest thanks and gratitude go to the love of my life, Oya, who has been the reason I started this challenging road in the first place. Your love and belief in me have been my inspiration to work hard and find a place in life. Your support and existence made this journey bearable. Your light that shines upon me has been my guidance through the end of the tunnel, which also forged our bond beyond. I am forever grateful to have you beside me.

Through the support of loved ones, I am more than happy to have started this unexpected journey that has made me realize the possibility of pursuing an academic career.

TABLE OF CONTENTS

ABSTRACT v

ÖZET iii

ACKNOWLEDGEMENTS v

TABLE OF CONTENTS vi

CHAPTER I 1

INTRODUCTION 1

1.1. Research Objective 3

1.2. Thesis Structure 5

CHAPTER II 7

LITERATURE REVIEW 7

2.1. Room Acoustics Parameters 7

2.1.1. Sound Absorption Coefficient (α) 8

2.1.2. Reverberation Time (RT60) 8

2.1.3. Speech Transmission Index (STI) 10

2.2. Previous Studies on Classroom Acoustics 10

2.3. Sound Absorbing Materials 12

2.3.1. Conventional absorbers 13

2.3.2. Resonant absorbers 15

2.3.3. Micro-Perforated Panels (MPPs) 17

2.3.3.1. Organic-Based Micro-Perforated Panels (Organic MPPs) 22

2.3.3.2. Inorganic-Based MPPs 26

CHAPTER III 29

METHOD 29

3.1. Design of the Research 29

3.1.1. Research Questions 30

3.1.2. Flow of the Study 31

3.2. Manufacturing Methods 31
3.2.1. Design of MPPs........ 32
3.2.2. Fused Deposition Modelling (FDM) Method 34
3.3. Measurements 40
3.3.1. Stage II-A: Impedance tube method (TS EN ISO 10534-2:2023)........ 40
3.3.2. Reverberation time (RT30) measurement method (TS EN ISO 3382-2:2008) 41
3.3.2.1. Stage II-B: In-situ measurement 41
3.3.2.2. Stage II-C: Acoustic simulation measurement........ 44
CHAPTER IV 47
RESULTS........ 47
4.1. Impedance Tube Measurement Results........ 47
4.2. In-situ Measurement Results........ 49
4.2.2. Reverberation Time (RT30) 49
4.2.3. Speech Transmission Index (STI) 50
4.3. Acoustic Simulation Measurement Results........ 50
4.3.1. Reverberation Time (RT30) 50
4.3.2. Speech Transmission Index (STI) 52
CHAPTER V........ 54
DISCUSSION 54
5.1. Micro-Perforated Panel (MPP) Performance 54
5.2. Objective Acoustic Parameters Results........ 56
5.3. Contribution to Interior Applications 58
5.4. Limitations 59
CHAPTER VI 61
CONCLUSION........ 61
6.1. Implications........ 61
6.2. Further Studies 62
BIBLIOGRAPHY 63

LIST OF TABLES

Table 1. STI evaluation with respect to ranges (Zhang et al., 2021).......................... 10
Table 2. Sound absorbing material categories (Adapted from Fuchs, 2013 and Fasllija, 2024).. 13
Table 3. MPP parameters (MPP1: PLA Panel, MPP2: PET Panel) 34
Table 4. Details of the 3D printing process (FDM) parameters 38
Table 5. Absorption coefficient of surfaces and materials in the room in 1/1 octave bands 46
Table 6. Converted absorption coefficients in 1/1 octave bands................................ 51
Table 7. STI values for each receiver in the room, compared with before and after treatments 53

LIST OF FIGURES

Figure 1. Optimal RT60 (in seconds) for room functions and volumes (Adams, 2016) 9
Figure 2. Membrane panel parameters (Left) and Helmholtz resonator parameters (Middle and Right), (Fasllija, 2024) 16
Figure 3. MPP parameters (Sakagami et al., 2009) 17
Figure 4. Absorption coefficients of an MPP (❑) (*d*=0.45 mm) and a Perforated panel (❍) (*d*=3 mm) resonators (*t*=3 mm) (*p*=1.4%) and (D=50 mm) (Fuchs, 2013) 18
Figure 5. Acrylic glass micro-perforated panels (MPPs) installed in the plenum of Bonn Parliament Building, Germany (Fuchs & Zha, 1997) 19
Figure 6. A micro-perforated foil used as a courtyard canopy at the German Historical Museum, Berlin, Germany (Left); A micro-perforated PVC membrane on the restaurant ceiling of the Modern Art at the Museum of Modern Art (MoMA), New York, USA (Right) (Adams, 2016) 20
Figure 7. Materials of porous sound absorbers (Adapted from Li & Ren, 2011) 22
Figure 8. Life cycle of a PLA-based product (Peng & Sun, 2017) 23
Figure 9. SEM images of coconut fiber and PLA MPP (BC-MPP) (Left and Middle); SEM image of steel MPP (Right), (Chin Vui et al., 2022) 25
Figure 10. Research procedure chart 30
Figure 11. Flowchart of the methods 31
Figure 12. MPP samples with back cavity distances (D) of 80, 60, 40, 20 mm in order (Left); Back cavities placed on their respective configuration (Right) 33
Figure 13. Drawing of the MPP with geometric parameters 33
Figure 14. Cross-sectional isometric view (Top); Cross-sectional view in right-side view of the sample drawing (Bottom) 35

Figure 15. Schematic demonstration of Fused Deposition Modelling (FDM) (Adapted from Mogan et al., 2023) ... 36
Figure 16. QIDI Tech X-Max 3 3D printer used to manufacture samples ... 36
Figure 17. An imperfect sample caused by a malfunctioned print (Left); A sample with unprinted holes (Right) ... 37
Figure 18. A heavy-duty drill press machine used to refine unprinted holes ... 39
Figure 19. Final state of four equal sections (a, b, c, d) on inhomogeneous MPP1 and MPP2 ... 40
Figure 20. TestSense impedance tube at BLX Acoustic Research Lab (İzmir, Türkiye) ... 41
Figure 21. In-situ measurement instruments in the classroom ... 42
Figure 22. Position of the source and receivers in the classroom ... 43
Figure 23. The positions of the sound source and the receivers are shown in the ODEON simulation 3D model, the same positions as the in-situ measurement ... 45
Figure 24. Position of the source and receivers with MPP allocation in the simulation ... 46
Figure 25. The absorption coefficients (α) of MPP1 at 1/3 octave bands ... 48
Figure 26. The absorption coefficients (α) of MPP2 at 1/3 octave bands ... 49
Figure 27. RT30 values for in-situ measured and simulated measurement results compared to the optimum value ... 50
Figure 28. Alpha values of sound-absorbing materials within the room in 1/1 octave bands ... 51
Figure 29. Measured and simulated RT30 results compared with MPP1 and MPP2 acoustic treatments ... 52
Figure 30. The absorption coefficients (α) of MPP1 and MPP2, at 1/3 octave bands, compared with the acrylic inhomogeneous MPP in the prior study by Fasllija (2024) ... 55

LIST OF ABBREVIATIONS

3D: 3-Dimensional

AM: Additive Manufacturing

BC-MPP: Bio-Composite Micro-Perforated Panels

C50: Clarity

ECM: Equivalent Circuit Method

EDT: Early Decay Time

FDTD: Finite Difference Time Domain

FDM: Fused Deposition Modelling

GA: Geometric Acoustics

MPP: Micro-Perforated Panel

NFRC-MPP: Natural Fiber-Reinforced Composite Micro-Perforated Panels

NRC: Noise Reduction Coefficient

NC30: Noise Criteria 30

PET: Polyethylene Terephthalate

PLA: Polylactic Acid

RT: Reverberation Time

TFM: Transfer Function Method

STI: Speech Transmission Index

SNR: Signal to Noise Ratio

CHAPTER I

INTRODUCTION

In architectural spaces, sound vibrations that reach our ears at different times affect our auditory perception (Fowler, 2016). People perceive the auditoria, the acoustic quality of a space, in three parts, in order: aesthetically, which depends on architectural design; ergonomically, shaped by its spatial arrangement; and functionally, determined by how efficiently sound waves travel within the acoustic environment (Fuchs, 2013). Acoustic design should always be considered during the design process, as it is difficult to change the shapes and dimensions of a room. Consequently, architects and acousticians during the design process should work in collaboration to provide livable spaces (Egan, 2016).

As part of the everyday experience, living rooms, offices, restaurants, and every type of room that has a function can be acoustically satisfactory or unsatisfactory (Kuttruff, 2006). Most notably, our ears may recognize unsatisfactory acoustic environments that are related to speech intelligibility and noise, commonly heard in educational environments (Sato & Bradley, 2008; Astolfi et al., 2012; Arvidsson et al., 2021). In these environments, both external and internal noise significantly affect elementary school students' academic performance in subjects such as mathematics, science, and literacy (Shield & Dockrell, 2008). Excessive reverberation times can create background noise, which can decrease the educational process and affect reading scores (Bradley & Sato, 2008). Additionally, these effects on background noise and reverberation can have long-lasting effects on students' well-being in classroom environments, such as changes in attitude and negative social interactions (Minelli et al., 2012).

When sound waves travel within the room and encounter rigid surface materials like stone, glass, metal, plaster, and wood, most of the sound is reflected, which can negatively impact acoustic quality and comfort if not controlled (Cox & D'Antonio, 2017). Considering both objective and subjective parameters of a room, architects and interior designers can make informed decisions to design a satisfactory acoustic environment.

One of the most important factors when designing a satisfactory acoustic space is controlling Reverberation Time (RT). Reverberation refers to the persistence of sound within a space until the source no longer generates sound (Egan, 2016). It is notably significant in various interior spaces, such as auditoriums, concert halls, offices, and classrooms. This optimal reverberation time is dependent on the room function. For example, a concert hall requires a longer reverberation time compared to an office, in order to improve the musical experience. Conversely, speech-related spaces such as offices and classrooms require shorter reverberation times to have clear speech intelligibility (Kuttruff, 2006; Barron, 2010).

Sound-absorbing materials are the most essential architectural applications in controlling reverberation in various spaces. These acoustic treatments are comprised of porous and resonant absorbers to control sound in their respective frequency ranges (Fuchs, 2013). Passive traditional absorbers, such as fibrous materials, provide sound absorption in high frequencies with lightweight properties and cheap options (Zhang et al., 2023). To improve low-frequency absorption, resonant structures are commonly used in architectural and interior spaces (Fuchs & Zha, 2006). These structures are represented by mass-spring systems, designed to damp the resonant frequency. In the acoustics field, they are listed as membranes, Helmholtz resonators, slotted panels, perforated panels, and Micro-Perforated Panels (MPP) (Cox & D'Antonio, 2017). These absorbers are only effective in specific frequency ranges, which requires additional resources to widen their bandwidth.

Recently, various studies (Mosa et al., 2019; Fasllija et al., 2021; Fasllija & Yilmazer, 2023; Fasllija, 2024; Laly et al., 2024) have explored MPPs to further expand their absorption bandwidth. They have implemented adjustments to traditional MPPs, which introduced their multi-resonance peak behavior. Although the research area has shifted towards improving the bandwidth of MPPs, the manufacturing techniques from traditional manufacturing methods like Computerized Numerical Control (CNC) to Additive Manufacturing (AM) processes are also investigated (Kazmer, 2017). AM, utilizing 3D printing, is implemented in various industries such as aerospace, automotive, medical, sports, and architecture. Specifically, in architectural applications (Salandin et al., 2022), 3D printing has recently been explored. Moreover, the usage of resources like polymers and thermoplastics is popular due to the increasing demand for Fused Deposition Modelling (FDM) in these industries (Ngo et al., 2018).

Conversely, the conventional manufacturing industries combined with conventional materials are harmful to the environment (Arenas & Sakagami, 2020) and pose threats to public health (Qiu, 2016). New alternatives to conventional materials should be explored, as sustainable materials are usually made of natural or recycled resources, and their production requires minimal energy (Asdrubali et al., 2012). Recently, sustainable concerns have shifted towards acoustic materials used in interior spaces, specifically Micro-Perforated Panels (MPP) (Liu et al., 2017; Sailesh et al., 2021; Sekar et al., 2021a, 2021b, 2022; Cobo, 2021; Rezaieyan et al., 2024). The current explorative study is focused on comparing new alternatives to conventional materials used in MPPs and implementing them in classroom settings.

1.1. Research Objective

In the acoustics field, from an engineering perspective, resonant structures are engineered and validated through complex mathematical formulae and models. While their contributions are known, from an architectural perspective, it is essential to assess a material from the design process to manufacturing processes and applications in interior spaces. When space efficiency is prioritized, thinner and more compact absorber designs, rather than large, conventional porous and fibrous materials, can be considered (Fuchs, 2013). Furthermore, a potential new approach should investigate sustainable alternatives to MPPs while comparing mechanisms tested in prior studies (Fasllija & Yilmazer, 2023; Fasllija, 2024).

Consequently, the aim of the study is not merely to demonstrate that sustainable MPPs can function effectively, but to examine different materials' behavior under controlled conditions. In doing so, the study seeks to fill a gap in current literature: Although PLA and PET have been separately explored as viable panel materials (Sailesh et al., 2021; Sekar et al., 2021a; Iannace & Ciaburro, 2021), no direct comparative analysis has been conducted using identical geometric parameters in the same application context. By fabricating PLA-based and PET-based MPPs with identical inhomogeneous configurations via additive manufacturing and evaluating them through both laboratory testing and classroom simulations, this research provides a clear foundation for understanding the relationship between material properties and acoustic performance. In particular, it highlights how the use of sustainable materials translates into acoustic performance. The results are intended to inform both the academic discourse on sustainable acoustic materials and the practical decision-making of architects and interior designers working in educational settings.

The main objective of this study is to develop and comparatively assess sustainable MPP configurations to implement in classrooms without relying solely on the conventional thick fibrous absorbers. The investigation follows a comprehensive workflow that bridges modelling, experimental validation, and architectural application. First, MPP samples made from PLA and PET were designed with inhomogeneous configurations to achieve multi-resonance peaks, and manufactured using Fused Deposition Modelling (FDM), and tested in the laboratory using the impedance tube method in accordance with ISO 10534-2:2023. Next, their performance was examined in a real classroom environment through in-situ measurements and predictive simulations conducted in Odeon Room Acoustics Software, focusing on objective key parameters such as Reverberation Time (RT30) and Speech Transmission Index (STI).

1.2. Thesis Structure

The thesis is organized into six main chapters. It starts from the literature-based foundations of the study with Chapter I, Introduction, and Chapter II, Literature Review. Through the experimental and analytical stages of Chapters III and IV, to the discussion of results and their broader implications in Chapters V and VI. Following the introduction, which sets out the acoustic challenges in classroom environments and situates the MPP mechanism within the broader shift toward sustainable materials, Chapter II presents a comprehensive literature review. This review covers fundamental concepts in room acoustics, including key parameters such as reverberation time and speech intelligibility, before examining the performance characteristics of porous and resonant absorbers. Special emphasis is placed on the theoretical basis of MPPs, recent innovations aimed at bandwidth improvements, and developments in manufacturing technologies, particularly additive manufacturing. The chapter concludes with an examination of sustainable MPP materials, highlighting PLA and PET as the samples for comparative evaluation.

Chapter III details the research method. It describes the design of the inhomogeneous MPP samples, the selection and preparation of PLA and PET materials, and the additive manufacturing process with trial-and-error experiments. The chapter outlines the procedures for laboratory testing using the impedance tube method in accordance with ISO 10534-2:2023, as well as the in-situ classroom measurements of RT30 and Speech Transmission Index, following ISO 3382-2:2008. The section also explains the setup of in-situ measurement instruments and calibration of predictive simulations in Odeon Room Acoustics Software, preserving the consistency between measured and simulated conditions.

The results are presented in Chapter IV, which reports the sound absorption coefficients of the PLA and PET panels across the 1/3 octave band spectrum, followed by the in-situ and simulated objective parameter results for the classroom environment. The findings are illustrated through graphs and tables to enable direct comparison between the two materials and to highlight frequency-dependent performance variations.

Chapter V provides a critical discussion of these results in light of previous studies. It analyzes the performance differences between PLA and PET in relation to their material properties, the implications for addressing low and mid-frequency reverberation problems, and their practical advantages and limitations in classroom applications. The chapter also considers the environmental significance of adopting biodegradable and recycled materials in acoustic treatment.

Finally, Chapter VI presents the conclusion, summarizing the main findings, discussing their implications for both acoustic design and sustainability, and identifying potential avenues for future research. By preserving this structure, the thesis maintains a logical flow that links the original research problem to its experimental exploration, and further, to the practical and theoretical contributions derived from the findings.

CHAPTER II

LITERATURE REVIEW

2.1. Room Acoustics Parameters

Room acoustics refers to the behavior of sound in an enclosed space and plays a critical role in determining how sound is perceived by users. Egan (2016) emphasized that any acoustical situation involves three key components: the source, the transmission path, and the receiver. These components are interconnected with the physical characteristics of a room, such as its shape, size, and surface materials. Sound waves produced in a room travel across a medium (most likely air) and interact with physical barriers, leading to variations in sound propagation, reflection, and dissipation. These acoustic phenomena produce a combination of diffused, reflected, absorbed, and direct sound energy. Physical characteristics of the room and sound movement in a medium impact the reverberation and overall acoustic quality of an enclosed space (Egan, 2016). The International Standards Organization defines the measurement of room acoustic parameters in three room types: performance spaces (ISO 3382-1: 2009), ordinary rooms (ISO 3382-2: 2008), and open plan offices (ISO 3382-3: 2022). Objective acoustic parameters such as Early Decay Time (EDT), Reverberation Time (T60), and Definition (D50) are used to evaluate acoustic quality based on impulse response measurement (ISO 3382-1:2009).

For ordinary rooms like classrooms, architectural design should include an optimal environment for concentration and speech. Reverberation Time (RT20, RT30, RT60) is the main parameter for evaluating acoustic quality in these spaces. There is growing interest in incorporating national standards with additional parameters such as Clarity (C50), Signal-to-Noise Ratio (SNR), and the Speech Transmission Index (STI) to better evaluate the acoustic environment, especially in educational settings (Daniels & Bodkin, 2015). Conventionally, in ordinary rooms, the primary objective acoustic parameter checked is Reverberation Time (RT60) for the sound energy to decrease 60 dB (Arvidsson et al., 2021). However, previous literature recommends increasing the Early Reflection Ratio or Clarity (C50) instead of reducing reverberation time in speech-related rooms (Bradley et al., 2003). Furthermore, Reverberation Time is typically the focus parameter in ordinary rooms where the objective is to reduce excessive reverberation by installing sound-absorbing materials. A balance between sound absorption proportion and audible speech level is necessary for a satisfactory sound environment (Sato & Bradley, 2008).

2.1.1. Sound Absorption Coefficient (α)

To reduce reverberation time and improve the acoustic environment, it is necessary to increase the use of sound-absorbing materials. Absorptive surfaces minimize unwanted sound reflections, controlling the reverberant sound field (Kuttruff, 1991). The sound absorption coefficient is specific to each material and represents the ratio between the sound energy incident on the surface and the absorbed sound pressure (Egan, 2016). The sound absorption coefficient (α) ranges from 0 to 1, where 0 indicates no absorption, and 1 represents perfect absorption within the frequency range of 125 to 8000 Hz (Egan, 2016).

2.1.2. Reverberation Time (RT60)

Reverberation Time (RT60) is when the sound energy level decreases by 60 dB (Barron, 2010). Formulated initially by Sabine (1923), RT60 is a key parameter for evaluating acoustic quality in rooms designed for speech purposes. The time it takes for the sound energy level to decrease depends on the overall sound absorption, material type, and material size. Sound-absorbing materials reduce a portion of the sound energy, thereby affecting the reverberation time. Sabine stated that reverberation in a room is influenced by two variables: the volume (V) and the total absorption of materials in the room ($\sum A$). He expressed the relationship between these variables using the following formula multiplied by the Sabine constant (0.16):

$$RT60 = 0.16\frac{V}{\sum A} \tag{2.1}$$

∑A = Total absorption of materials = $A_1 * \alpha_1 + A_2 * \alpha_2 + \ldots + A_n * \alpha_n$

In most cases, RT60 is used instead of RT30 for reverberation time measurements because generating a source signal 60 dB above the background noise is difficult. RT60 is defined as twice the time it takes for sound levels to drop from -5 dB to -35 dB. This value derives from the 60 dB reduction in sound level, hence corresponding to RT60 (Adams, 2016; ISO 3382-2: 2008).

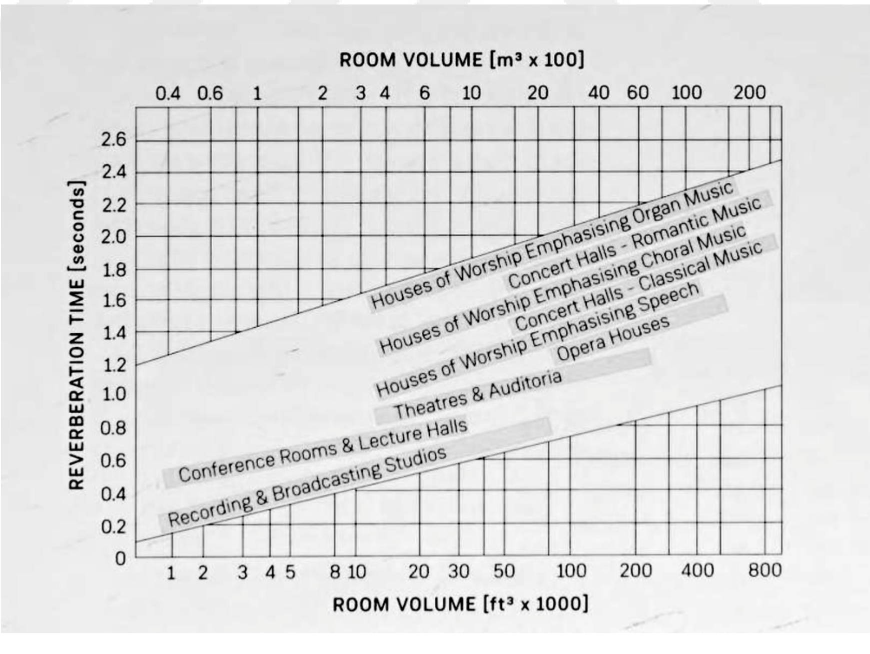

Figure 1. Optimal RT60 (in seconds) for room functions and volumes (Adams, 2016)

The optimal RT60 value for a space should be determined with respect to its function. Figure 1 illustrates appropriate reverberation time ranges and respective functions with their volumes. For instance, the optimum RT60 value for rooms with speech purposes is 0.2-1.3 s, while for music-related rooms, RT60 should range between 1.4-2.4 s. Excessive reverberation is controlled through various acoustic treatments, such as using absorbers and diffusers. Sound absorbers work in lowering the reverberant sound levels, while sound diffusers evenly distribute sound energy in the room (Cox & D'Antonio, 2017). Various systematic approaches aimed at acoustic design and acoustic treatments in auditoria of medium-sized acoustic environments used for speaking and collaboration (Bistafa & Bradley, 2000; Choi, 2013; Sanavi et al., 2017; Cucharero et al., 2019; Labia et al., 2020; Zhang et al., 2021; Selim & Saeed, 2022).

2.1.3. Speech Transmission Index (STI)

In unfavorable conditions, reflections that arrive late to the listener are perceived as echoes, whereas in favorable conditions, they are contributors to reverberation in a room. Theoretically, any reverberation tends to reduce speech intelligibility by distorting its timing and blending the spectral characteristics of consecutive phonemes or syllables (Kuttruff, 2006). To predict speech intelligibility through an objective measurement method, Steeneken & Houtgast (2002) have developed the metric of Speech Transmission Index (STI) that ranges on a scale from 0 to 1, as shown in Table 1. Depending on the reverberation and clarity of the speech signal across speech frequencies, STI values should be higher than 0.64 in lecture halls, classrooms, and meeting rooms for good speech intelligibility (Labia et al., 2020).

Table 1. STI evaluation with respect to ranges (Zhang et al., 2021)

STI ranges	0.00-0.30	0.30-0.45	0.45-0.60	0.60-0.75	0.75-1.00
Evaluation	bad	poor	fair	good	excellent

2.2. Previous Studies on Classroom Acoustics

In speech auditoria, such as meeting rooms and classrooms, it is essential to maintain the consistent voice of the speaker. This is dependent on Reverberation Time (RT60), and measurable with Speech Transmission Index (STI) (Astolfi et al., 2012). Therefore, to control excessive vocal effort within a classroom and control RT60, total sound absorption within the room should be sufficient (Labia et al., 2020). Consequently, previous literature implemented absorbing and diffusing acoustic panels (Choi, 2013; Iannace et al., 2013; Sanavi et al., 2017; Campbell et al., 2019; Selim & Saeed, 2022) and investigated auditoria using Finite Difference Time Domain (FDTD) simulation (Bistafa & Bradley, 2000; Buratti et al., 2016; Fratoni et al., 2019; Cucharero et al., 2019; Labia et al., 2020; Zhang et al., 2021).

Choi (2013) investigated periodic-type diffusing and absorbing panels in a 1/10 scale physical classroom model. Reverberation Time (RT30) results showed that a combination of absorption and diffusion on the ceiling surface, with a portion on the front wall, provided better and consistent RT30 results in all frequencies and improved Clarity (C50). In addition to these objective parameters, the Speech Transmission Index (STI) is essential for investigation within a classroom. Sanavi et al. (2017) assessed objective room parameters, including STI and RT20. The STI values for the current room condition yielded a “good” score (0.70). They implemented a “Class A” absorbing panel, which exceeds the perfect absorption ratio of 1 after 500 Hz. Subsequently, RT20 was decreased to a range of 0.4-0.6s at 500-1000 Hz. Similarly, in another study (Campbell et al., 2019), a “Class A” glass wool absorber was installed on three walls with an area of 8 m2, achieving RT20 levels of around 0.6s 125-4000 Hz. However, an extended acoustic treatment of good sound absorbers may result in overdamping, which may diminish the propagation of useful sounds (Labia et al., 2020).

Buratti et al. (2016) compared recycled sound absorbers in a lecture room simulation while evaluating their Life Cycle Assessment (LCA). The average RT60 and STI values of the real room were measured as 2.5s and 0.43. They introduced different configurations of recycled absorbers with varying geometric parameters. The best absorption performance was observed in a configuration with glass wool and scraps of wastepaper mixed. The treatment reduced RT60 values to 0.7-0.8s while improving STI to a 0.75 score. Additionally, LCA evaluation showed that this solution allowed a cost saving of 68%. Similar studies (Iannace et al., 2013) implemented natural-based materials like fabric-covered jute bag panels within classrooms to add a function to the space while improving the acoustic performance.

Fratoni et al. (2019) utilized an FDTD simulation using ODEON Acoustics Simulation Software, investigating six large lecture halls in a university. Such acoustic software is used to predict and validate the measured objective parameters of a room. They validated STI and RT20 results with measured ones. The aim of their study focused on the impact of room volume, placement, and the area of sound-absorbing surfaces. Furthermore, other related studies focused on the absorbing material amount and placement while considering the right configurations to avoid overdamping of the sound (Cucharero et al., 2019; Labia et al., 2020).

2.3. Sound Absorbing Materials

Considering the objective assessment of a room, if the reverberant sound is dominating the sound environment, the application of sound-absorbing materials becomes essential. Sound-absorbing mechanisms are effective in reducing the reverberant sound (Kuttruff, 1991). When sound waves travel through a medium, the sound energy is absorbed, reflected, and transmitted to an absorbing material. The sound absorption coefficient of a material is measured to determine whether that material is efficient at absorbing sound. This value is the ratio between the absorbed acoustic pressure and the incident energy (Egan, 2016). The ratio varies from 0 to 1, respectively, indicating no absorption to perfect absorption in frequencies of 125-8000 Hz.

This section categorizes sound-absorbing materials as shown in Table 2. It introduces two main categories classified by their mechanisms: conventional absorbers and resonant absorbers. Although a resonating mechanism, Micro-Perforated Panels (MPP) are explained separately in Section 2.3.3, which is the focus of this study.

Table 2. Sound absorbing material categories (Adapted from Fuchs, 2013 and Fasllija, 2024)

	Material	Mechanism	Frequency range (Hz)	Examples (in Figures)
Porous / Fibrous	Foams Rockwool Perlite	Friction Heat	Mid to high 1000-8000 Hz	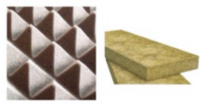
Membrane	Rubber Vinyl	Mass-spring	Low 50-500 Hz	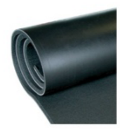
Helmholtz Resonator	Wood Concrete Masonry block	Mass-spring	Low to mid 300-1000 Hz	
Micro-Perforated Panels	Acrylic Metal	Mass-spring	Low to mid 300-1000 Hz	
Acoustic Metamaterials	3D printed materials	Tunable	Low to mid 300-1000 Hz	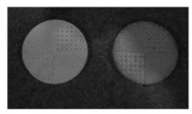

2.3.1. Conventional absorbers

Conventional sound-absorbing materials such as mineral wool, rock wool, fiberglass, drywall, textiles, curtains, carpets, and foams are the most common acoustic materials used in interior spaces. These materials consist of porous or fibrous passive absorbing properties, which are most effective at diminishing high-frequency noises (Kumar & Lee, 2019). Porous and fibrous materials absorb sound energy through two mechanisms: soft materials absorb sound due to deformation caused by the impact of sound, while porous materials absorb sound by the vibration of the air inside their pores and lose energy through friction (Gonzalez, 2019). Li & Ren (2011) stated that the sound absorption coefficient of these materials is affected by several factors.

The sound absorption of porous materials depends on their high porosity. Materials with a greater number of smaller and open pores perform better in terms of sound absorption. Their physical structure consists of many interconnected pores and bubbles that run from the surface through the inner parts, allowing air permeability. However, if the surface is sealed with a dense layer or if the material becomes wet, the absorption performance would be greatly reduced (Li & Ren, 2011). Under these conditions, they are protected with fabric, membranes, or perforated plates. Though they should not be covered with rigid materials that hide porous or fibrous surfaces completely (Gonzalez, 2019).

Density significantly impacts sound absorption, as density increases, materials tend to absorb sound better in lower frequencies, while their high-frequency performance decreases drastically (Li & Ren, 2011). Consequently, an optimal density value exists for any material. If the density exceeds a certain point, the material gains excessive rigidity and performs more like a solid rather than a fibrous material, losing its air permeability (Gonzalez, 2019). The high porosity of these materials provides intrinsically high air content. They have an acoustic impedance (Z) that is very similar to that of air (Z_{air}). This means that when a sound wave hits the surface, most of its energy tends to be absorbed, and only a small fraction is reflected.

Further, an increase in the thickness of a porous material improves its performance in absorbing low-frequency sounds (Cox & D'Antonio, 2017). In contrast, this increase has a very minimal effect on its absorption performance in high-frequency sounds. Theoretically, a material of infinite thickness would be the perfect sound absorber (Gonzalez, 2019). Like the density factor, the actual thickness is limited to a certain point. In practice, they have a finite depth and are typically mounted on a reflecting surface. Therefore, an incident sound wave that is not immediately absorbed must traverse the material twice. First, the waves must pass through the material and then reflect from the back surface. Throughout this trip, the sound energy is progressively dissipated through interactions with the material's structure, mainly caused by friction and deformation (Gonzalez, 2019). Furthermore, rather than increasing the material thickness, an air cavity at the back of the material is more effective, which improves sound absorption in low frequencies (Li & Ren, 2011).

Conventional materials or porous absorbers can be classified according to their microscopic structures as cellular, fibrous, or granular. A common characteristic of these materials is a permeable surface that allows the penetration of incident sound waves. Cellular materials like open-celled polyurethane and foams are made of interconnected small openings. Fibrous materials are characterized by tunnel-like parallel openings formed between natural or synthetic fibers, such as those of glass and mineral fibers. Granular materials consist of larger, solid particles packed together with minimal empty space between them. These materials include asphalt, concrete, clays, sands, gravel, and soils (Arenas & Crocker, 2011).

Most commercially available porous sound absorbers, like mineral wool, fiberglass, gypsum, and foam, are made of fibrous composition. Fibers are classified as either natural or synthetic (artificial). Natural fibers can be derived from plants (cotton, kenaf, hemp, wood, etc.), animals (wool, fur, felt), or minerals (asbestos). Synthetic fibers include minerals (fiberglass, glass wool), polymers (polyester, polypropylene), or cellulose (bamboo fiber). These synthetic mineral and polymer fibers are commonly used for thermal insulation, as well as sound absorption. When combined with more than one component material, they are often referred to as composites (Arenas & Crocker, 2011). Composites involve soft textiles as coverings to conventional absorbers, or a back cavity is filled with a soft material to broaden its effective frequency range (Gonzalez, 2019). However, their manufacturing requires high-temperature industrial processes and chemicals derived from oil, which can be harmful to the environment and potentially pose health risks, including eye and skin irritation (Qiu, 2016). Furthermore, their end-of-life disposal poses great challenges for waste management (Arenas & Sakagami, 2020).

2.3.2. Resonant absorbers

Conventional porous absorbers are usually placed at the room boundaries, where the particle velocity is zero, and surfaces furthest from the back cavity are most effective. This inefficiency is rooted in the requirement for large thicknesses of materials, which diminishes overall absorption performance (Padhye & Nayak, 2016). To achieve broadband passive absorption across all frequencies, resonant and porous materials are integrated together. Additionally, mechanisms such as Helmholtz Resonators, Membrane Panels, and Micro-Perforated Panels are superior in achieving greater absorption in lower frequencies (Cox & D'Antonio, 2017). Resonant mechanisms act as a mass and a spring system. Their design allows for a tunable resonant frequency, which can suppress unwanted sound propagation and reduce excessive reverberation (Liu et al., 2017).

In membrane panels, the mass is the air in the opening of a perforated sheet. The back cavity (D) acts as the spring against the mass, that is, the sound waves flowing in the air (Cox & D'Antonio, 2017). However, Helmholtz resonators have a different mechanism with a narrow neck (Figure 2). Sound waves enter through this neck and travel through friction, inside the back cavity, losing their energy while being absorbed (Egan, 2016). Though this mechanism works in a very limited frequency range, it is possible to make it most effective in low frequencies by having a large back cavity volume (*V*), a long neck length (*l*), and a smaller perforation size (*d*) (Gonzalez, 2017).

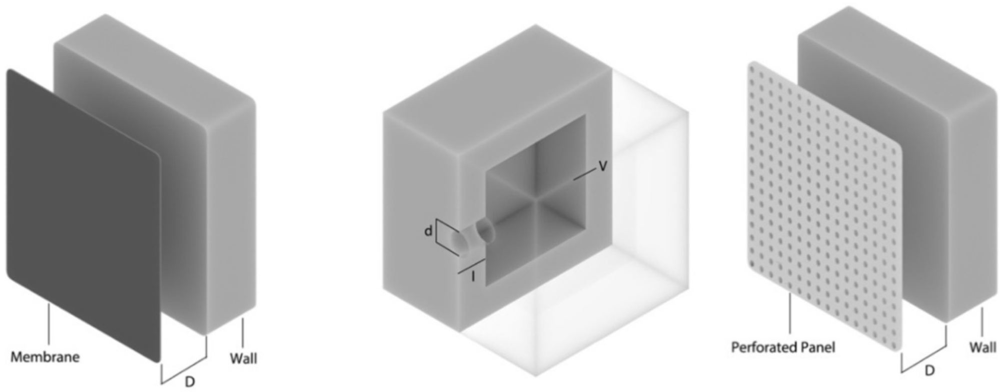

Figure 2. Membrane panel parameters (Left) and Helmholtz resonator parameters (Middle and Right), (Fasllija, 2024)

2.3.3. Micro-Perforated Panels (MPPs)

Theorized by Maa (1975), Micro-Perforated Panels (MPP) are known for their ability to absorb sound energy with sub-millimeter perforated holes and mechanisms to control low-frequency resonance. This model eliminates the necessity of using inherently porous or fibrous materials in the air cavity behind the panel, as the sound is damped with the viscous boundary effect. Geometric parameters shown in Figure 3, such as hole diameter (*d*), panel thickness (*t*), perforation ratio (*p*), and air cavity depth behind the panel (*D*), can be modified to adjust the acoustic efficiency of the system. They can also be efficient in any desired frequency range through various design configurations by changing the parameters (Fuchs, 2013).

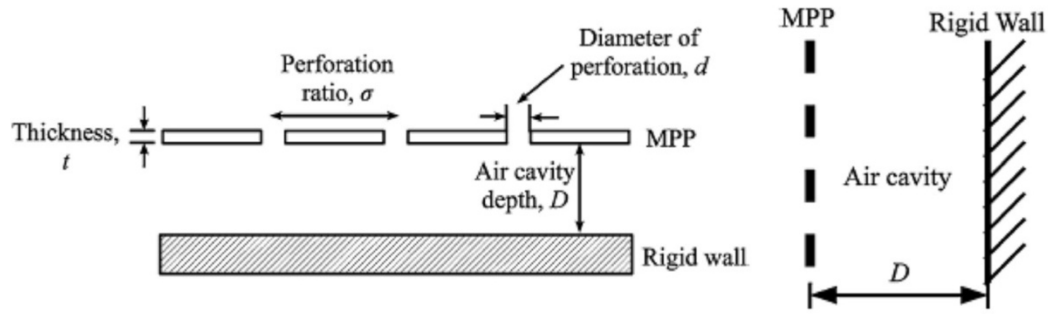

Figure 3. MPP parameters (Sakagami et al., 2009)

For optimum efficiency, Fuchs and Zha (1997) provided estimations based on a computer program and verification with the standing wave tube (ISO 10534-1: 1996) and reverberation room measurements (ISO 354: 2003). They argued that the acoustic efficiency of the MPP slightly depends on the panel material and its physical characteristics. The most important requirement for the system to work is to diminish vibrations caused by the sound energy. Such vibrations disrupt the absorption mechanism and are caused by lowering the velocity of the vibrating air travelling through the micro-holes of the panel due to the viscous boundary effect. Thus, MPPs are most efficient when the particle velocity is high in the perforations (Herrin et al., 2017). For the optimum effectiveness in the system, hole diameters should range from 0.1 to 2 mm, and the distance between holes should be 2-20 mm. Most efficient panel thicknesses range from 0.2 to 30 mm; for larger dimensions, mechanical strength and stiffness need to be considered (Fasllija, 2024). Fuchs and Zha (1997) tested different air cavity depths and verified 25-100 mm to be ideal, with no distinction between open or closed lateral boundaries. In addition to altering the distance of these parameters, angled perforations (Liu et al., 2016; Sailesh et al., 2021), slit perforations (Cobo, 2021), inhomogeneous perforation sizes (Mosa et al., 2019; Fasllija et al., 2021; Laly et al., 2024), coiled perforations (Prasetiyo et al., 2021), and uneven back cavities (Sakagami et al., 2009; Ruiz et al., 2012; Fasllija & Yilmazer, 2023; Fasllija et al., 2024) are investigated in prior studies. The complex theorizing and modeling of these designs could cause an impractical process in architectural applications, as achieving satisfactory sound absorption performance is more crucial.

Despite their limited absorption bandwidth, MPPs are a more sterile, aesthetically pleasing, and efficient alternative to fiber and foam-based sound-absorbing materials. MPPs are often referred to as a pioneering sound-absorbing material that performs better in terms of absorption efficiency in the desired frequency bandwidth when compared to traditional perforated panels, as shown in Figure 4 (Fuchs & Zha, 1997; Maa, 1998; Kang & Brocklesby, 2005; Fuchs, 2013).

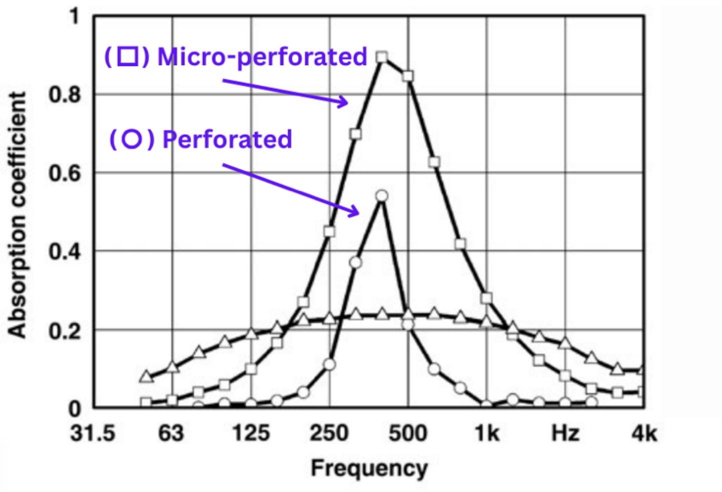

Figure 4. Absorption coefficients of an MPP (❑) (*d*=0.45 mm) and a Perforated panel (❍) (*d*=3 mm) resonators (*t*=3 mm) (*p*=1.4%) and (D=50 mm) (Fuchs, 2013)

The first generation of MPPs was made of metal and had circular laser-cut perforations, which is an expensive manufacturing method. Although the first generation of MPPs pioneered the next generation of MPPs in theory, they lacked practicality in interior applications. Unlike the first generation, second-generation MPPs are made of glass, carbon-fibers, and plant and animal-based materials and rely on less expensive manufacturing methods like etching, cutting, and shearing (Herrin et al., 2017). One of the first interior application examples of MPPs was done with acrylic glass panels (Figure 5) in the Parliament Building of Bonn, Germany (Adams, 2016). First trials included utilizing transparent convex plates; however, they produced unwanted optical reflections within the plenum. Each plane absorber, 1.2 m^2 in size, was fixed at an angle, with its back cavity varying from 20 to 75 mm. The final combination of these transparent panels included both absorbers and diffusers. Therefore, the diffusivity of the sound field inside the parliament is achieved while absorbing unwanted reverberation (Fuchs & Zha, 1997).

Figure 5. Acrylic glass micro-perforated panels (MPPs) installed in the plenum of Bonn Parliament Building, Germany (Fuchs & Zha, 1997)

Unlike the rigid materials mentioned above, more tensile and flexible materials like membrane and foil-type MPPs are also utilized in previous literature (Kang & Fuchs, 1999; Shen et al., 2022; Ciaburro & Iannace, 2022). A micro-perforated foil was installed in the courtyard canopy of the German Historical Museum in Berlin, Germany, with 1.15x1.15 m each attached to the corners of a wire mesh spanned across the glass roof, at a 15 cm back cavity (see Figure 6a). A similar design was implemented at a restaurant in the Modern Art at the Museum of Modern Art (MoMA), New York, USA. The design utilized a micro-perforated PVC membrane backed with fiberglass for a better absorption performance while stretching over the dining and bar area ceiling, imitating a white glass with sharp edges (Adams, 2016) (see Figure 6b).

Figure 6. A micro-perforated foil used as a courtyard canopy at the German Historical Museum, Berlin, Germany (Left); A micro-perforated PVC membrane on the restaurant ceiling of the Modern Art at the Museum of Modern Art (MoMA), New York, USA (Right) (Adams, 2016)

In addition to large-scale architectural applications, MPPs have also been investigated in interior spaces (Cingolani et al., 2021; Fasllija, 2024) along with perforated panels (Pereira et al., 2021) using predictions with Finite Difference Time Domain (FDTD) and Geometric Acoustics (GA) simulations. In one of the recent interior application examples, Fasllija and Yılmazer (2023) compared inhomogeneous parallel-arranged MPPs in a classroom/meeting room of Bilkent University. Utilizing the Equivalent Circuit Model (ECM), four panels with different perforation sizes were implemented to the same MPP, arranged in parallel, like an electric circuit. This inhomogeneous design was proposed to achieve a broader absorption bandwidth, specifically in the low-frequency range. Additionally, they combined inhomogeneity with multiple-layer MPPs by comparing single-layer and double-layer MPPs. Initially, different materials like fiber cement and ABS

(Acrylonitrile Butadiene Styrene) were tested for rigidity and aesthetic purposes. Then acrylic glass, a commonly used transparent material in interior spaces, was adopted for the base material of the samples. The micro-perforations were traditionally manufactured utilizing CNC (Computerized Numerical Control) with perforations varying from 0.7 to 2 mm and 6 mm thickness for all panels. According to ISO 10534-2: 2023, the absorption performance of MPPs was measured using TFM (Transfer Function Method) in an impedance tube, and then, objective parameters were compared with ODEON Acoustics Simulation Software. Their alpha values were compared across different configurations for optimal broadband absorption. Reverberation Time (RT60) and Speech Transmission Index (STI) results showed a significant improvement compared to surface impedance predictions based on the computerized algorithm of Maa's Theory (1975, 1998) in MATLAB R2020a. The results were aligned with the theory while achieving a broader absorption bandwidth, thanks to a parallel arrangement (Fasllija & Yılmazer, 2023). Furthermore, multiple-layer MPPs are investigated to achieve a wider absorption bandwidth through Maa's (1998) double-layer proposal (Ruiz et al., 2011; Cobo & Simon, 2019; Cobo et al., 2019; Yang et al., 2020).

Although the sound absorption performance of MPPs is not directly related to the type of material, rather their surface characteristics, like porosity and flow resistivity, can change absorption and reflection performance (Adams, 2016; Cox & D'Antonio, 2017). Supposing that the rigidity of the material is retained, MPP principles can be integrated into various materials, including metal, wood, glass, and plastics. This diversity allows interior designers and architects to combine aesthetic concerns with acoustic efficiency in built environments (Fuchs, 2013). Moreover, different conventional construction materials are also practiced in MPPs, such as acrylic glass (Fuchs & Zha, 1997; Asdrubali & Pispola, 2007; Sakagami et al., 2021; Fasllija & Yılmazer, 2023), gypsum-based materials (Aslan & Turan, 2020), foam-based materials (Patil et al., 2024), wood-based materials (Sheng & Mo, 2010; Xu et al., 2018), and metal-based materials (Arjunan et al., 2021). However, recent studies have shifted towards replacing these materials with sustainable alternatives (Asdrubali, 2012). In terms of the manufacturing process, organic and inorganic MPPs cause minimal impact on the environment compared to the conventional materials mentioned above.

2.3.3.1. Organic-Based Micro-Perforated Panels (Organic MPPs)

Organic or natural materials are derived from plant-based and animal-based polymers, which most commonly have fibrous characteristics (Figure 7). Fibrous sound resonance structures achieve a broader bandwidth of absorption than traditional fibrous sound absorbers (Zhang et al., 2023). Organic-based composite materials, often called Natural Fiber-Reinforced Composite Micro-Perforated Panels (NFRC-MPP) or Bio-Composite Micro-Perforated Panels (BC-MPP). Natural fibers such as wood fiber (Sekar et al., 2021a) and corkwood (Rezaieyan et al., 2024), kenaf, and coconut fiber (Chin et al., 2018; Chin Vui et al., 2022), and sugarcane (Beheshti et al., 2024) are made into composites using polylactic acid (PLA) as a thermoplastic base for binding the fibers together.

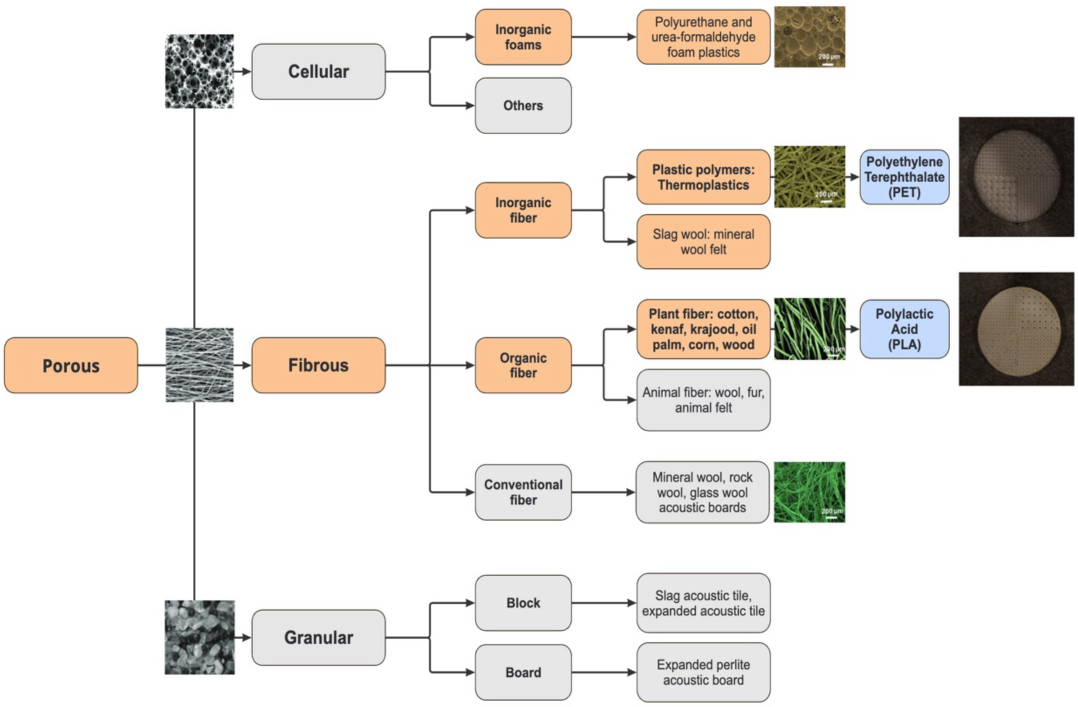

Figure 7. Materials of porous sound absorbers (Adapted from Li & Ren, 2011)

PLA is one of the most common biodegradable materials, produced from lactic acid obtained through the fermentation of corn, potatoes, sugar, and sugar beets (Sailesh et al., 2021; Sekar et al., 2021a). As seen in Figure 8, the life cycle of PLA is initiated with photosynthesis from corn plants (1). Starch is extracted from corn (2) and its grains and then fermented to produce lactic acid (3), which is a one-component variation of polylactic acid (PLA). It is first produced in granular form (4) and then processed into the desired form to yield different products of PLA (5). After the products reach their end-of-life phase, PLA can be disposed of (6) with composting and is biodegraded into the environment (7). Moreover, the authors (Sekar et al., 2021b) studied the biodegradation process of 3D printed PLA and PLA reinforced oil palm fruit bunch fibers. The weight loss of the samples is compared as they start to wear and lose their polymer chains and degrade into carbon dioxide. After four weeks, the natural fiber with 40 wt.% PLA lost 21% of its weight, 12% higher than pure PLA. Recently, with the increased attention to 3D printing in manufacturing acoustic mechanisms, PLA is one of the more popular filaments (Peng & Sun, 2017).

Figure 8. Life cycle of a PLA-based product (Peng & Sun, 2017)

Sekar et al. (2021a) compared 3D printed PLA-MPPs reinforced with PLA-wood fiber filament. The sound absorption coefficient (α) of four samples with different geometric parameters was measured using an impedance tube. The sample with the least thickness (t = 2 mm) and perforation diameter (d = 0.2 mm) achieved the broadest bandwidth (1500-3500 Hz) while having the highest α value of 0.93 at 2173 Hz. The other three samples had their resonant frequencies in the middle of the 1000-2000 Hz range, with a peak α value of 0.73.

Rezaieyan et al. (2024) investigated 3D printed Natural Fiber-Reinforced Composite Micro-Perforated Panels (NFRC-MPPs) made of corkwood/PLA (30 wt.% corkwood) and compared them with base PLA-MPPs. Perforation diameters (d) varying from 0.6 to 1 mm, perforation spacing (b) 2 to 10 mm, material thickness (t) 0.6 to 1 mm, and back cavities (D) 30 to 70 mm, their Sound Absorption Coefficients (α) were measured using the impedance tube method. The alpha values at absorption peaks for d = 0.6 mm and d = 1 mm were 0.73 and 0.50, respectively, at 756 Hz and 922 Hz. The effect of perforation diameter (d) showed that as the perforation diameter decreases, alpha increases. Researchers discussed that as the perforation diameter (d) increases, peak absorptions are observed in the higher frequency range (Qian et al., 2013). Similarly, as perforation spacing (b) increased from 2 to 10 mm, α values drastically increased from 0.19 to 0.90 at 1595 Hz and 612 Hz. Thus, as the perforation distance increased, the absorption peaks started to shift towards higher frequencies. Conversely, at lower frequency ranges, greater α values are observed with the surface having a reduced perforation ratio (*p*) (Liu et al., 2017). The material thickness (t), varying from 0.6 mm to 1 mm, demonstrated that as the thickness increased, α values also increased accordingly, from 0.57 (at 906 Hz) to 0.73 (at 778 Hz). As expected from prior studies (Sakagami et al., 2008), a thicker panel caused the resonant frequency to shift towards the low frequency range. Conformably, as the back cavity (D) increased from 30 mm to 70 mm, α values slightly increased by 7.7 %. The perforation of the panel and air within the back cavity would represent acoustic mass and acoustic spring. Thus, a resonance shift towards higher frequencies is observed. The study is concluded by discussing the effect of material choice. NFRC-MPP (α = 0.88) achieved slightly greater absorption than PLA-MPP (α = 0.86). The results were attributed to the intrinsic network of the pores, meaning that as the porosity of fibers increases, sound absorption becomes superior (Chin et al., 2018).

Research conducted by Chin et al. (2018) compared Bio-Composite Micro-Perforated Panels (BC-MPPs) made of kenaf fiber and PLA resin. The samples were manufactured with mixing, drilling, and hot pressing. They are designed with different material compositions while retaining the physical MPP parameters at a constant (Sample diameter = 100 mm, t = 1 mm, d = 1 mm, p = 1). The lowest composition of kenaf fiber (5%) backed by a 10 mm air gap yielded similar results to the α values of base-PLA (α = 0.86). The samples with 30 wt.% kenaf fibers showed the highest α value of 0.99 at the 1521 Hz frequency. Therefore, because of the increased composition of kenaf fibers, there is an increasing network of loose natural fibers along with their porosity. Peak sound absorption occurs when the stiffness of the air gap (spring) removes the acoustic mass of the holes (mass) (Liu et al., 2017).

Additionally, comparisons between BC-MPPs and traditional MPPs are also investigated in prior studies (Chin Vui et al., 2022; Beheshti et al., 2024). The authors (Chin Vui et al., 2022) manufactured a coconut fiber mixed BC-MPP mixed with PLA in different proportions, increasing in 5% increments from 5% to 30%. The α results of configurations were compared with a conventional MPP made of steel. The BC-MPP showed a broader bandwidth while having greater α values than the steel MPP. Shown in Figure 9, the samples were examined closely with Scanning Electron Microscope (SEM) imaging, and BC-MPP was observed to have a very complex and tortuous structure, while for steel, it was nonexistent. Subsequently, the lack of a porous open-ended network of steel diminished its absorption properties, compared to porous fibers like coconut and PLA.

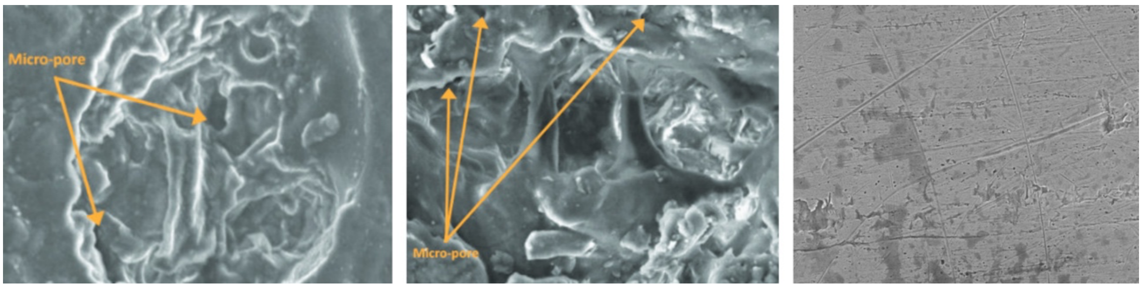

Figure 9. SEM images of coconut fiber and PLA MPP (BC-MPP) (Left and Middle); SEM image of steel MPP (Right), (Chin Vui et al., 2022)

Similarly, Beheshti et al. (2024) designed sugarcane-based Natural Fiber-Reinforced Composite Micro-Perforated Panels (NFRC-MPP) using polyvinyl alcohol (PVA) as an adhesive. Physical parameters of perforation diameter (d = 0.5 mm) and perforation ratio (p = 1%) remained constant, while the thickness of the plate (t) and the weight proportion (wt.%) of sugarcane were compared among NFRC-MPP configurations and conventional Plexiglass MPP. The samples with 8- and 10-mm thicknesses achieved a higher absorption across lower frequencies, while the peak α values are observed in samples with lower thicknesses. Overall, NFRC-MPP succeeded in superior α values compared to plexiglass, except with a thickness of 10 mm (at 1000 Hz), where it underperformed. Single-layer natural MPP with sugarcane felt as filler material in the back cavity yielded peak absorption (around α = 0.9) at 100 Hz. However, compared to single-layer ones, double-layer natural MPPs achieved slightly lower absorption (76%) across all frequencies while performing better in lower frequencies (160-200 Hz). The findings of the research concluded that the density and thickness of natural fibers impact sound absorption (Berardi & Iannace, 2015), while having multiple layers increases low-frequency efficiency. Additionally, natural fibers absorb sound better due to their inherently porous structure, which plexiglass does not possess.

2.3.3.2. Inorganic-Based MPPs

In the literature, inorganic and recycled absorbers are most popularly represented by plastic-based composites such as polycarbonates (Liu et al., 2016), polystyrene from recycled packaging manufacturers (PS) (Garcia-Valles et al., 2008), and recycled polyethylene terephthalate (PET) (Li et al., 2017; Iannace & Ciaburro, 2021), PET flakes and powder (Caniato et al., 2021; 2022), polyvinyl alcohol (PVA) (Shen et al., 2022), and synthetic panels (Homkhiew et al., 2024).

Though inorganic and synthetic materials are often paired with other non-natural chemical binders, in some cases, they are mixed with natural fibers. Homkhiew et al. (2024) investigated thermal conductivity and sound absorption performance of krajood fibers (organic) adhered with isocyanate glue (inorganic). Krajood fibers were used in the core layer, and for surface layers, wood-plastic composites were used. These materials were adhered as sandwich panels, which exhibit the highest α value of 0.78 at 1000 Hz. The outcome of the study recommended that the recycled polypropylene (PP) reinforced with krajood fibers could be implemented. Natural fibers are often comprised of a loose, porous network, which chemical binders could strengthen.

The authors (Liu et al., 2016) investigated 3D printed MPPs made of porous propylene polycarbonate mixed with salt. The impact of different perforation angles from 0 to 45 degrees was compared between air gap lengths while analyzing their Sound Absorption Coefficients (α). The most absorptive range among all samples was found to be 2000-4000 Hz with peak absorption at 3328 Hz. The findings indicated that as the perforation angle increased, absorption efficiency shifted towards lower frequencies. Consequently, as the air gap length increased, peak absorption at lower frequencies increased.

Li et al. (2017) manufactured flexible MPPs made of plastics: polyvinyl chloride (PVC), polyethylene terephthalate (PET), and polyimide (PI) using a Computer Numerical Control (CNC) milling machine. The first samples had varied parameters of perforation diameter (d = 0.085-0.1 mm), thickness (t = 0.1-0.3 mm), perforation distance (b = 0.42-0.86 mm), and perforation ratio (p = 1.06-4.55%) and were compared with Maa's Model. Though every sample achieved peak absorption at 3000 Hz, PET performed in a broader bandwidth. PET achieved the highest absorption peak, which is 10.6% higher than PVC at 1500 Hz. Then, the effect of structural parameters was investigated while changing the parameters in each case. The widest absorption bandwidth was observed in the PET sample with a configuration of d = 0.1 mm, t = 0.15 mm, b = 0.63 mm, p = 1.96%, and back cavity length (D) of 15 mm. The researchers concluded that better absorption properties are due to better mechanical properties, such as toughness, elasticity, and flexibility.

Increased porosity means increased flexibility, which greatly improves the absorption of sound energy (Asdrubali et al., 2012). Researchers (Shen et al., 2022) implemented a flexible membrane MPP comprised of polyvinyl alcohol (PVA). The sample showed greater absorption in all frequencies, compared to Maa's Theory. The study's outcome suggested that with the appropriate geometric parameters and porosity, composites with other materials are not necessary. This highlights the potential to explore non-composite materials for further studies.

Conversely, porous acoustic panels made of PET flakes and powders were investigated as composite alternatives for recycled acoustic materials (Caniato et al., 2021; 2022). PET bottles and rigid expanded polystyrene (PS) were ground to be foam materials that possess a cellular form. PET flakes at the bottom and PET/PS powders were placed at the top of the sample. However, this method was found to be inconsistent by the authors, as achieving homogeneous flake distribution is a tedious process. Every side with different proportions of chemicals like alginate, glycerol, and PET powder/flake variations was compared in terms of their sound absorption. All the samples achieved an exponential growth of absorption towards high frequencies. The researchers found that these materials are tunable, depending on the type and shape of the microplastic. Additionally, an increased proportion of alginate improved the acoustic performance and stiffness, as it behaves like a binder to the foam structure (Caniato et al., 2022).

Similarly, Iannace & Ciaburro (2021) investigated the acoustic properties of PET panels with a Gaussian regression model. Recycled PET bottles were shredded and converted into a granular form. Then, they were bound through a hot rolling press. Their α values were compared with thicknesses varying from 10 mm to 60 mm. The panels that are thicker than 40 mm showed superior absorption (α values close to 1) and wider absorption bandwidth at 1000-1800 Hz.

CHAPTER III

METHOD

3.1. Design of the Research

The study aims to explore new material alternatives to conventional ones used in MPPs while comparing them in interior spaces. The research procedure is shown in Figure 10 and summarized as follows:

The initial phase focused on the parametric design of micro-perforated panel (MPP) configurations using inhomogeneous arrangements to achieve multi-resonance peak absorption. These designs were informed by the Electric Equivalent Circuit Model (ECM).

In the second phase, MPP samples were manufactured with sustainable materials: biodegradable polylactic acid (PLA) and recycled polyethylene terephthalate (PET), and via additive manufacturing (AM) with Fused Deposition Modelling (FDM). Laboratory testing was carried out using an impedance tube in accordance with ISO 10534-2:2023 to obtain absorption coefficients across a wide frequency range.

The third phase involved application in a classroom setting, where in-situ acoustic measurements of Reverberation Time (RT30) and Speech Transmission Index (STI) were conducted both before and after the installation of the panels. These measurements were verified by predictive simulations in Odeon Room Acoustics Software, allowing for the calibration of a geometric acoustic model of the space.

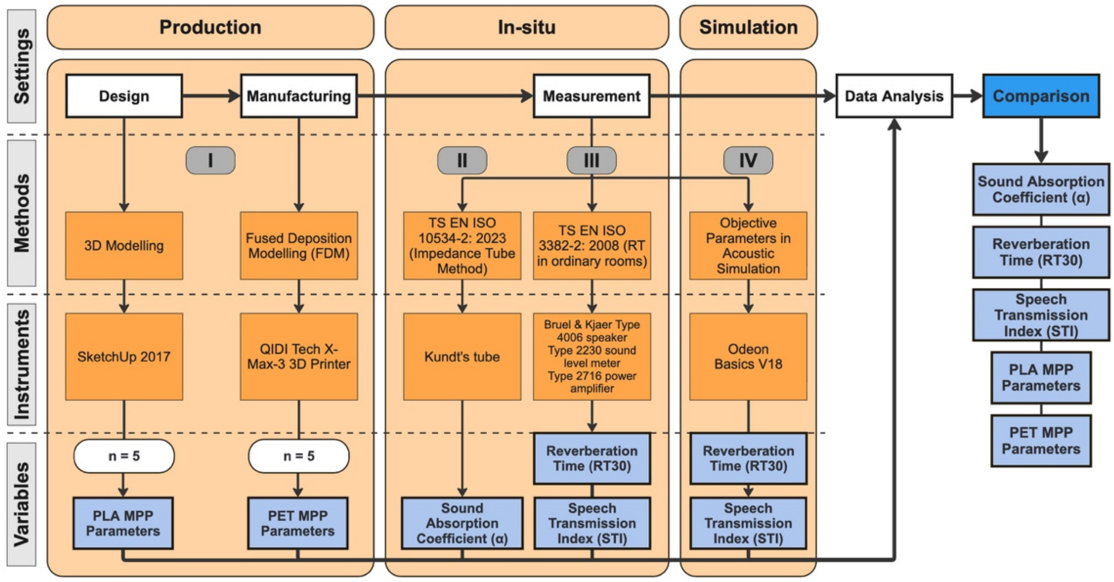

Figure 10. Research procedure chart

3.1.1. Research Questions

This research has one main research question and a hypothesis based on assumptions considering observations from previous studies:

Research Question: Is there a significant difference between the sound absorption performance of PLA-based MPP (MPP1) and PET-based MPP (MPP2)?

Hypothesis: The acoustic performance of PLA-based MPP (MPP1) in improving RT30 and STI is better than that of PET-based MPP (MPP2).

3.1.2. Flow of the Study

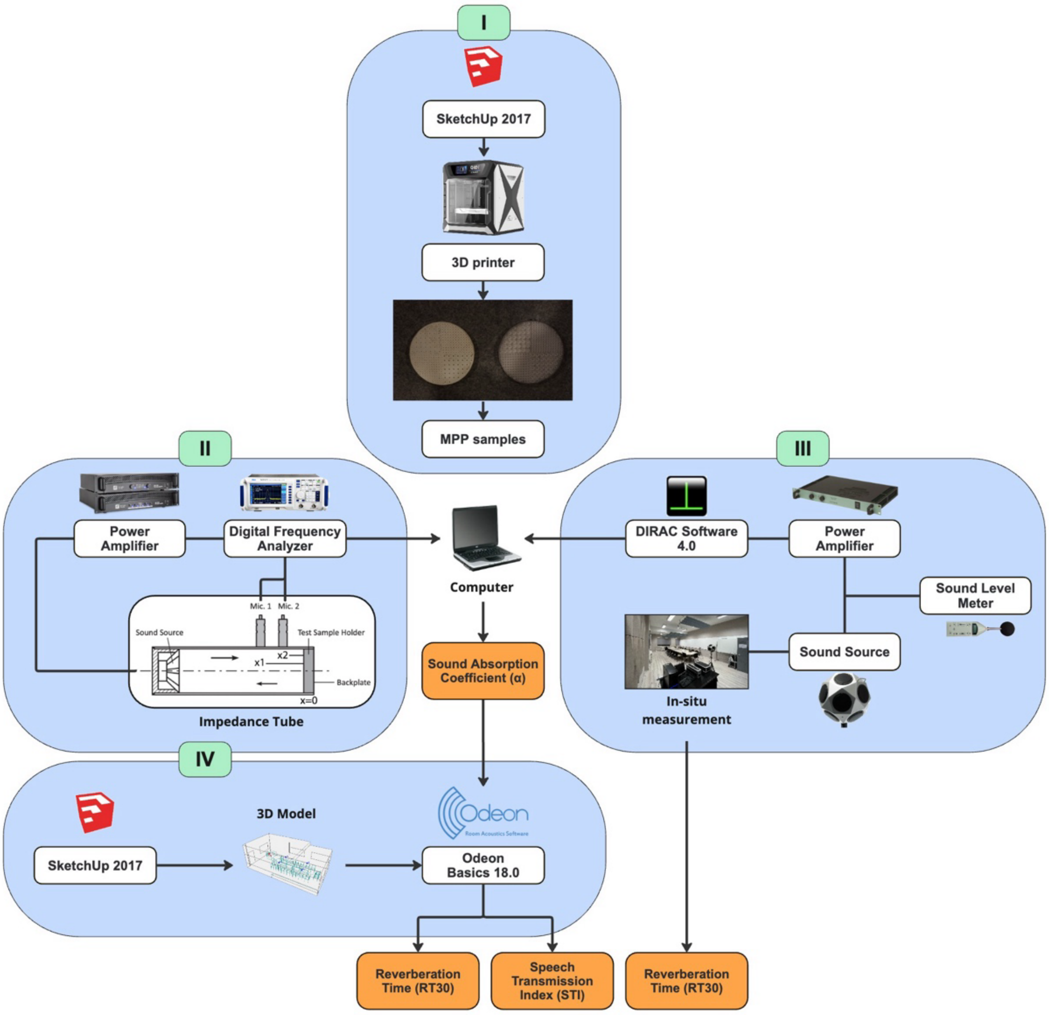

Figure 11. Flowchart of the methods

3.2. Manufacturing Methods

3D printing processes are a class of Additive Manufacturing (AM) that provides a flexible design without compromising material quality and minimal resource management (Kazmer, 2017). Processes utilizing 3D printing are comprised of: Stereolithography (SLA), Selective Laser Sintering (SLS), Fused Deposition Modelling (FDM), and Polyjet Modelling (PJM). The most commercially available and cheap option among them is FDM. Additionally, their material inventory consists of thermoplastics like acrylonitrile butadiene styrene (ABS), polylactic acid (PLA), and polycarbonate (PC), which are known for their cheap and designable features. Consequently, in the scope of the study, FDM was preferred to manufacture samples.

In contrast to expensive traditional MPP manufacturing methods such as Computerized Numerical Control (CNC) (Fasllija & Yılmazer, 2023; Fasllija, 2024), Infiltration Method (Cobo & Montero De Espinosa, 2013), Selective Laser Sintering (SLS) (Yang et al., 2020), and Digital Light Processing (DLP) (Carbajo et al., 2024), 3D printing allows for inexpensive precision manufacturing without compromising quality. Recently, research on 3D printing has become popular on acoustic materials often used in interior spaces, specifically Micro-Perforated Panels (MPP). Prior studies utilized 3D printing to manufacture MPPs, specifically implementing FDM (Liu et al., 2017; Sailesh et al., 2021; Sekar et al., 2021a, 2021b, 2022; Cobo, 2021; Rezaieyan et al., 2024).

3.2.1. Design of MPPs

Previous studies compared parallel and serially arranged panels utilizing the Electric Equivalent Circuit Model (ECM). To align with the literature, Micro-Perforated Panels (MPP) were designed as inhomogeneous, which equally divided a panel into four parts with different perforation sizes and ratios. The MPP parameters were selected for the most efficient acoustic performance in low to mid frequencies, according to satisfactory comparisons with ECM (Fasllija & Yilmazer, 2023; Fasllija, 2024). The flow of the methods is illustrated in Figure 11.

The sample thickness (*t*) of configurations (a, b, c, d) was set constant at 6 mm-thick circular PLA (density = 1240 kg/m^3) and PET (density = 1270 kg/m^3) panels. Appropriate for an impedance tube measurement, the samples were designed circular with diameters of 100 mm and 30 mm. Cavity distances (D) of 80, 60, 40, and 20 mm in order are shown in Figure 12. Other geometric parameters like hole diameter (*d*) and perforation ratio (*p*) are listed in Table 3. The first set of samples (MPP1) shows the configurations and parameters related to PLA-based MPPs, and the second set (MPP2) shows the former and latter related to PET-based MPPs (Figure 13). Guided by observations made from prior studies, the geometric parameters were set constant to align with prior studies while comparing the impact of material choice.

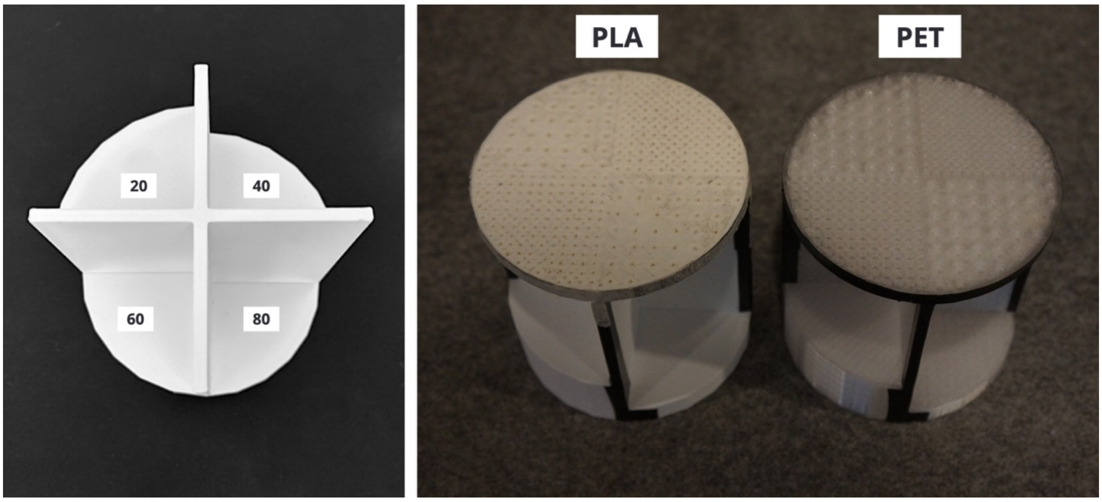

Figure 12. MPP samples with back cavity distances (D) of 80, 60, 40, 20 mm in order (Left); Back cavities placed on their respective plate configuration with different materials, respectively PLA and PET (Right)

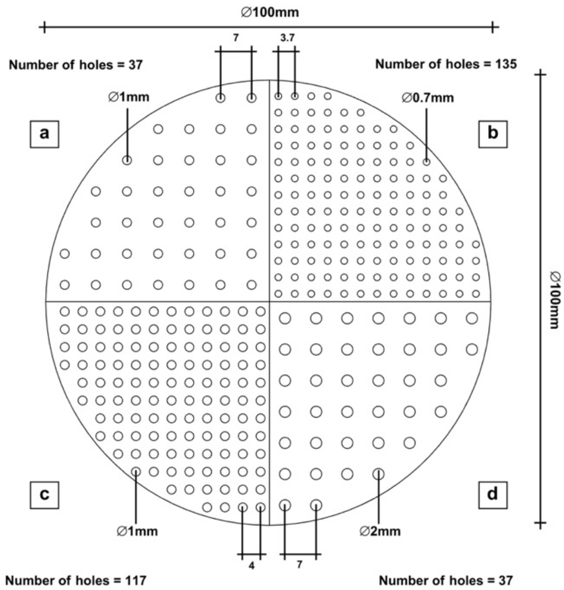

Figure 13. Drawing of the MPP with geometric parameters

Table 3. MPP parameters (MPP1: PLA Panel, MPP2: PET Panel)

Sample ID	***d (mm)***	***t (mm)***	***p (%)***	***D (mm)***
MPP1-a **MPP2-a**	1	6	1,6	80
MPP1-b **MPP2-b**	0,7	6	2,8	60
MPP1-c **MPP2-c**	1	6	3,14	40
MPP1-d **MPP2-d**	2	6	6,4	20

3.2.2. Fused Deposition Modelling (FDM) Method

To manufacture samples, as an organic material, Polylactic Acid (PLA), and as an inorganic material, Polyethylene Terephthalate (PET) were selected. These materials can be referred to as thermoplastics, which are commonly used in 3D printing (Mogan et al., 2023). They are comparable to the topics of previous studies in terms of their cost-effective manufacturing process and acoustic performance in architectural settings. Authors (Sekar et al., 2021a; Sailesh et al., 2021; Gautam et al., 2023; Rezaieyan et al., 2024) have argued that PLA is biodegradable with industrial composting methods and has poor strength but good flexibility for 3D printing (Sailesh et al., 2021). PLA filament and derivatives can be shaped at 200-230 °Celsius temperatures in the nozzle of a 3D printer. Moreover, it is a lightweight and low-cost material fit for composites and PLA matrices (Stoof et al., 2017).

On the other hand, PET is slightly more durable than PLA and is more resistant to heat, which can be shaped at 225-260 °Celsius temperatures. One of the most commercially common plastic polymers (thermoplastics), PET, is obtained from recycled empty bottles, which requires 60% less energy compared to a newly produced material (Iannace & Ciaburro, 2021). PET and its derivatives in inorganic thermoplastics are easier to procure since they require fewer chemical interventions to be molded into printable filaments. PET is not utilized in 3D printing as much as PLA and Acrylonitrile Butadiene Styrene (ABS), and other thermoplastics like polycarbonate (PC), Polyether Ether Ketone (PEEK), and Nylon are used at a minimum in composites (Mogan et al., 2023). There is a lack of prior studies related to the use of PET as an acoustic material, specifically with FDM. Consequently, a comparison with a more popular polymer (PLA) used in FDM was convenient within the scope of the study.

Initially, the samples were virtually modeled using SketchUp Version 2017, and the 3D models were exported into a slicer software (Ultimaker Cura 3D Printing Software Version 5.8) as an STL (Stereolithography) file. The models were then inspected with a cross-section to validate solidity before they were exported (Figure 14).

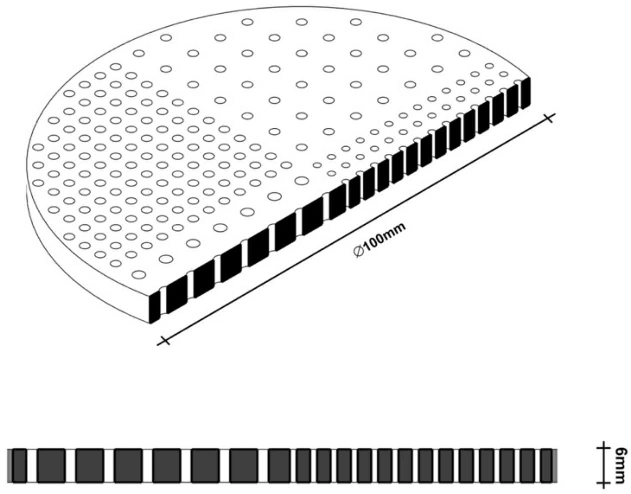

Figure 14. Cross-sectional isometric view (Top); Cross-sectional view in right-side view of the sample drawing (Bottom)

The manufacturing process is performed with the Additive Manufacturing (AM) method, which utilizes Fused Deposition Modelling (FDM) in 3D printing. Throughout the manufacturing process, this method achieved precision micro-perforations without changing nozzle tips. The steps followed in the FDM that consist of the 3D printing process are illustrated in Figure 15.

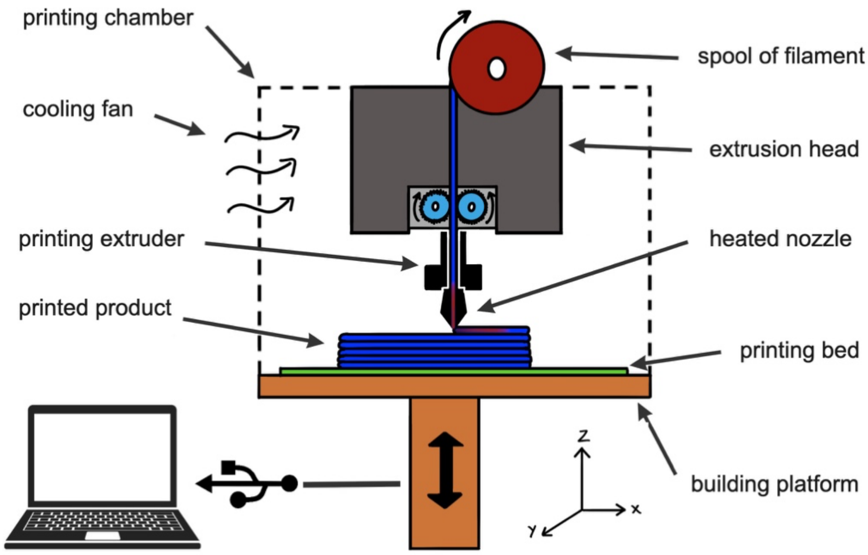

Figure 15. Schematic demonstration of Fused Deposition Modelling (FDM) (Adapted from Mogan et al., 2023)

Figure 16. QIDI Tech X-Max 3 3D printer used to manufacture samples

The samples were printed using a commercial-grade QIDI Tech X-Max 3 3D printer (Figure 16), which heats filaments and extrudes outputs through the nozzle. The printing chamber is dimensioned at 325x325x315 mm. The outputs were structured with 1.75 ± 0.5 mm-thick layers and built on the printing bed. This part of the printer is constantly heated to prevent the outputs from getting stuck on the surface of the bed. The required bed temperature range for PLA filament is 60-75 °Celsius, and for PET filament, 70-90 °Celsius. Finding the appropriate temperatures for melting the filament is a significant part of the preparation phase, since underheating or overheating could result in filament clogging inside the nozzle, which could cause the printer to malfunction and cause imperfections in the samples. Figure 17, on the left, shows the result of a malfunctioned printing process, particularly caused by clogged PLA filament. Freshly obtained PET and PLA filaments were carefully selected, as any moist or spoiled filament can cause a malfunctioned print. The PET filament was heated and printed at 250 °C nozzle temperature, while the PLA filament was at 220 °C. The printing bed temperature for both filaments was carefully selected after trial-and-error while following the recommended temperature range. The bed temperature for PLA MPP (MPP1) was set to 60 °C, and the bed temperature for the PET MPP (MPP2) was 75 °C. To prevent overheating within the chamber, the cooling fan was turned on during the printing process, especially for PET filaments, since they require more heat for printing. Overall, PET filament was printed faster than PLA filament, but the curing process remained the same. Table 4 details the printing parameters of samples related to the manufacturing process mentioned above.

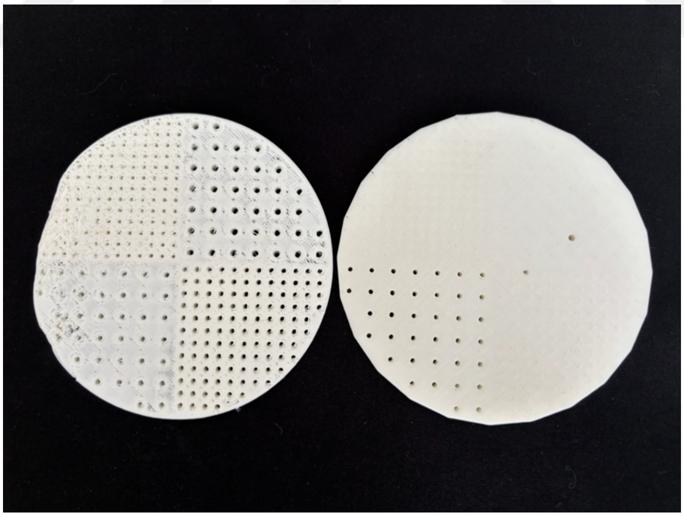

Figure 17. An imperfect sample caused by a malfunctioned print (Left); A sample with unprinted holes (Right)

Table 4. Details of the 3D printing process (FDM) parameters

Printing parameters	**Materials**			
	PLA MPP	**PET MPP**	**PLA Cavity**	**PET Cavity**
Infill percentage (%)	20%	20%	10%	10%
Required nozzle heat (°C)	220	250	220	250
Required bed heat (°C)	60	75	60	75
Filament used (g)	37.13	33.81	150	154
Print time (h, min)	3 h 4 m	2 h 38 m	7 h 45 m	7 h 42 m
Section view	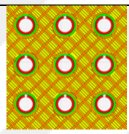	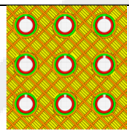	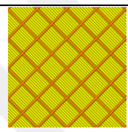	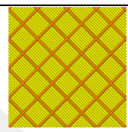

Additionally, higher extruder speeds can cause errors in keeping the chamber cool enough for an adequate printing process while heating the filament at a constant temperature. Underheating the filament caused each printed layer to cool down and block the previous layers; as a result, sub-millimeter holes could not be printed, as shown in Figure 17, on the right. To eliminate this obstacle, a drilling press machine was used in the Department of Mechanical Engineering Laboratory at Bilkent University. Unprinted holes were manually drilled using a Sharp Heavy Duty Drill Press Machine SE-330BF to ensure every hole is visible from both sides, prior to measurement (Figure 18). Following a recommendation from previous literature (Mogan et al., 2023), a faster printing time is compromised to eliminate this printing limitation, and the extruder speed was set to a medium-high speed, constant at 100 mm/s. After the preparations, the extruder started printing the first layer, drawing the boundaries of the workspace. The remaining void between the boundary was filled with a zig-zag infill pattern until reaching the maximum height. A trial-and-error approach was followed to determine the most efficient sample infill density and infill geometry for a satisfying structural integrity while maintaining the printing process steadily fast. The initial samples were tested respectively in 40%, 20%, 15%, 10% and 8% infill percentages. The 20% and 15% variations provided fast print times while they remained structurally strong and preserved their absorbing characteristics. Prior studies (Sekar et al., 2022) found that greater densities could undermine porosity and sound absorption ability. The back cavity modules (PLA Cavity, PET Cavity) were printed with 10% infill density. Any larger densities were not needed for structural integrity since the back cavity modules were only needed as solid backings.

Figure 18. A heavy-duty drill press machine used to refine unprinted holes

To align with previous literature (Fasllija & Yilmazer, 2023; Fasllija, 2024), the sample size was set to five for each type of sample to ensure that the sampling error is less than 5%. The printer was able to produce five samples from 1/5 (20 wt.%) of one spool (1 kg) of each PET and PLA filament. In total, 20 wt.% filament was used from 2 kg of filament. Initial print tests for MPP1 (PLA) and MPP2 (PET) showed that their surface characteristics were different. MPP2 resulted in a smoother finish while MPP1 showed millimetric porous imperfections. Subsequently, the post-printing process involved sanding the samples using 1000-grit sandpaper to keep the surfaces smoother, so that an appropriate sound incidence inside the impedance tube is achieved. This adjustment was not aimed at making the surface characteristics of the two materials the same, but rather to trim the imperfections caused by printing. Finally, to clean the particles left over from sanding, every sample was sterilized and wiped with alcohol before the impedance tube measurement (Figure 19).

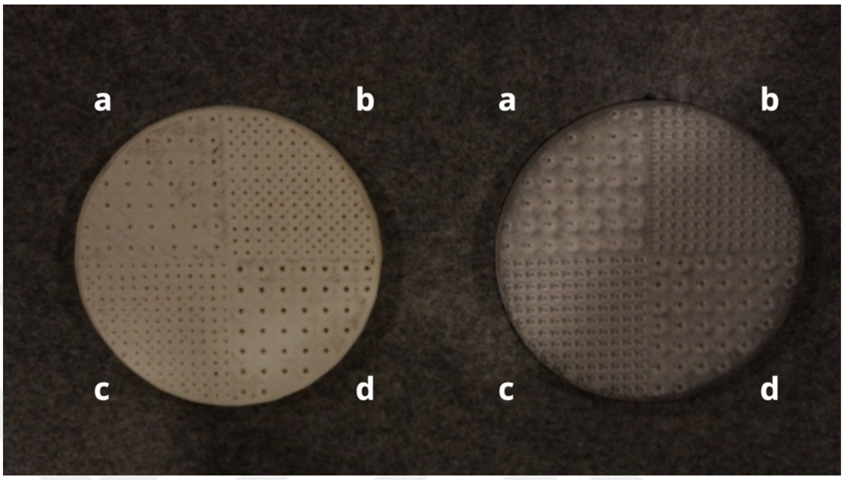

Figure 19. Final state of four equal sections (a, b, c, d) on inhomogeneous MPP1 (PLA) and MPP2 (PET)

3.3. Measurements

3.3.1. Stage II-A: Impedance tube method (TS EN ISO 10534-2:2023)

To follow measurement procedures and align with previously used methods (Fasllija & Yilmazer, 2023; Fasllija, 2024), this phase involves the first step of the measurement process to obtain the Sound Absorption Coefficient (α) inside a Kundt's impedance tube according to TS EN ISO 10534-2 (2023), utilizing the Transfer-Matrix Method (TMM). The samples were measured in BLX Acoustic Research Lab, an accredited acoustic measurement laboratory located in Izmir, Türkiye. The experiment was performed using a TestSense Impedance Tube, a domestic tool. Prior to the experiment, the speaker and two microphones inside the tube were calibrated in idle conditions, as shown in Figure 20. The room temperature and humidity were relatively stable at 22° Celsius and 44%. For accurate results, the samples were securely placed and sealed inside the tube using electric tape to prevent any air leakage. The measurement procedure was performed as follows: a sound signal from the speaker was sent inside the tube. Following the sample at the other end of the tube, sound energy was absorbed. This was calculated by measuring sound pressure generated by the microphones, 100 mm apart from each other, and the sound absorption coefficient was obtained (ISO 10534-2, 2023). Traditional to the standard, sound absorption coefficient measurement results are obtained within the frequency range of 63-1600 Hz (for a 100 mm sample) and the 1600-4000 Hz frequency range (for a 30 mm sample) in 1/3 octave bands. For comparability to previous literature, only 100 mm samples were used to assess the absorption effectiveness in the low-frequency range. To increase the reliability of sample results, each measurement was repeated three times with five samples for each material type.

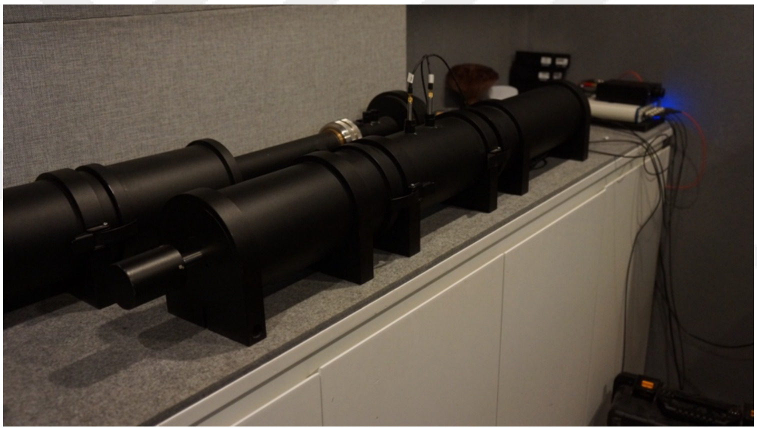

Figure 20. TestSense impedance tube at BLX Acoustic Research Lab (İzmir, Türkiye)

3.3.2. Reverberation time (RT30) measurement method (TS EN ISO 3382-2:2008)

3.3.2.1. Stage II-B: In-situ measurement

To assess the acoustic performance of the research samples in a simulated environment, first, the objective acoustic parameters were measured in the research setting. The in-situ measurement was performed in a classroom at the Department of Interior Architecture and Environmental Design at Bilkent University. To achieve a uniform result, the experiment was done on a Saturday afternoon with no classes occurring, as depicted in Figure 21. The room is a designated classroom for the department's graduate students. It resides in a relatively desolate area in terms of sound intensity, though outdoor noise caused by traffic can be a distracting factor inside the classroom. The room is dimensioned at 10.12 m in length and 5.47 m in width, with a height of 3.6 m. The furniture consists of a 15-person wooden meeting table and fabric-covered wooden chairs with no heavy drapery on the windows. Overall, the absorption area in the room is very limited, except for fabric-covered panels used on the right-hand wall. To address this issue, an acoustic intervention was made in previous literature (Yilmazer et al., 2024).

Figure 21. In-situ measurement instruments in the classroom

An acoustic treatment was centered on improving the acoustic parameters of Reverberation Time (RT30) and Speech Transmission Index (STI). Initial results for STI scores were satisfactory, but RT30 values exceeded 2 s in low to mid frequencies, failing to satisfy the guidelines (Daniels & Bodkin, 2015). Rooms used for communication and education purposes, with a volume of less than 250 m^3, RT30 should be lower than 0.6 s in the 500-1000 Hz frequency range (Yilmazer et al., 2024). Further, a subjective measurement was made to understand the soundscape, and researchers asked 90 meeting room users to assess Perceived Affective Quality (PAQ), a subjective method. The participants found the room “dynamic,” “annoying,” and “monotonous,” which supports the fact that the acoustic performance of the classroom is not sufficient even after the treatment (Yilmazer et al., 2024).

Four cracker cloud panels as suspended ceiling elements and six absorber panels made from recycled PET and mixed with felt fibers were implemented to improve the acoustic performance in the classroom. The PET-based material's Noise Reduction Coefficient (NRC) was 0.75 (Yilmazer et al., 2024). After the treatment, RT30 values decreased to a 1 s average. In terms of speech intelligibility, the Speech Transmission Index (STI) showed an improvement from "fair" with 0.48 average score to 0.62, resulting in "good" intelligibility in the meeting room (Zhang et al., 2021; Yilmazer et al., 2024).

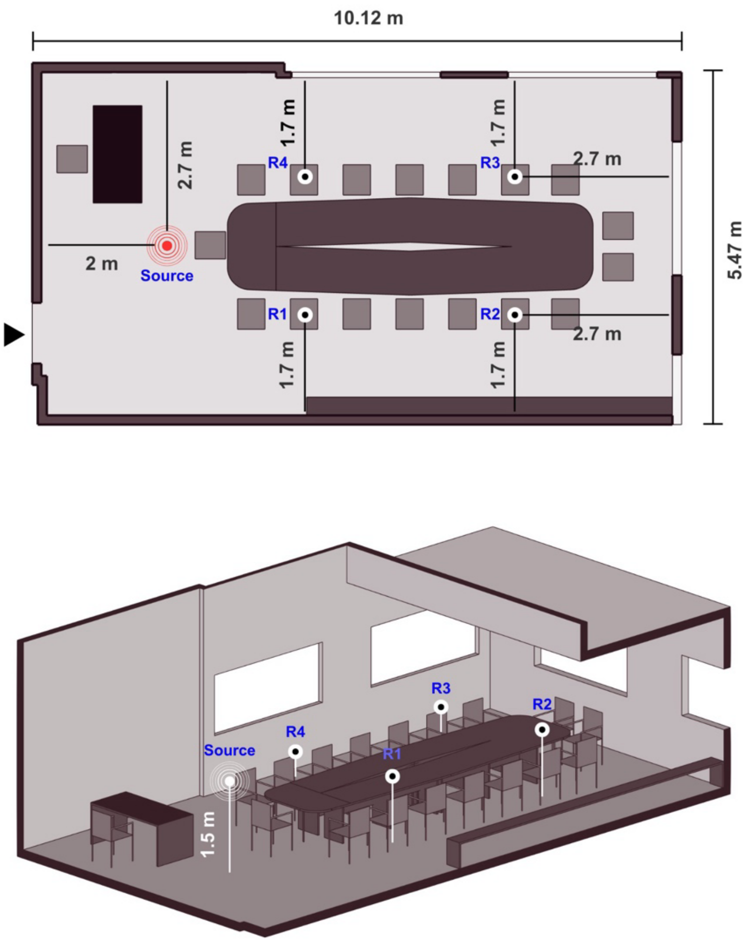

Figure 22. Position of the source and receivers in the classroom

The only sound source was placed 2 m in front of the whiteboard and 2.7 m from the right-hand wall, facing the audience. Four receivers were located 1.7 m x 2.7 m away from the walls. The height of the sound source was considered as 1.5 m, mouth height at standing position, while receivers were placed at 1.2 m height at sitting position (Figure 22). Following the TS EN ISO 3382-2:2008, RT30 measurement was initiated using the DIRAC version 4.0 Acoustic Analyzer Software. A sound signal was sent from this software, using a Bruel & Kjaer Type 4006 omnidirectional speaker powered by a B&K power amplifier type 2716. The signal was sampled at 44 kHz and processed with the sound card of an HP Compaq nx9005 laptop. An impulse response was obtained as a sound file, which yields RT30 results. The sound signal was recorded at a closer perimeter to the sound source using a B&K 2230 sound level meter. The average value of the background noise level was 38 dBA, which falls below the recommended maximum noise level of 45 dBA for unoccupied classrooms in Türkiye (Çevresel Gürültünün Değerlendirilmesi ve Yönetimi Yönetmeliği, 2022).

3.3.2.2. Stage II-C: Acoustic simulation measurement

In a simulated environment, a 3D model of the classroom was created using SketchUp Version 2017. Then, the model was imported into ODEON Basics Version 18.0 using the SU2ODEON plug-in. The 3D modeling followed the recommendations for geometrical acoustics that specify surfaces must be larger than 0.35 m (Vorlander, 2020). The positions of the sound source and the receivers remained the same following in-situ measurements (Figure 23). The sound file obtained from the impulse response of the in-situ measurement was used to calibrate the simulated environment. This adjustment was made to reflect the same acoustic conditions of the real environment for more reliable results in measuring objective acoustic parameters.

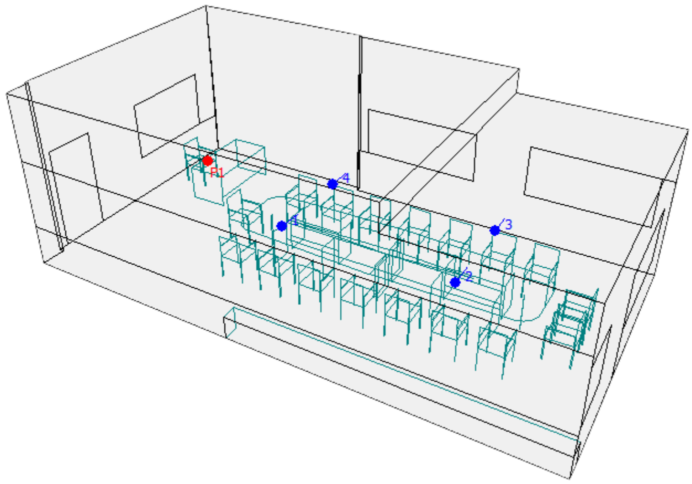

Figure 23. The positions of the sound source and the receivers are shown in the ODEON simulation 3D model, the same positions as the in-situ measurement

The Sound Absorption Coefficient (α) of materials regarding each surface was assigned based on recommendations in previous literature (Cox & D’Antonio, 2017; Vorlander, 2020; Christensen, 2023). The absorption coefficients were adjusted through a trial-and-error calibration process to achieve at least a 5% difference between measured and simulated RT30 values for each receiver (ISO 3382-2, 2008). The adjusted values of absorption coefficients (α) for each room surface type are shown in Table 5. The scattering coefficient was set constant at 0.01 for all surfaces of the room. To answer the research questions at hand, alpha values of PLA and PET MPPs (MPP1, MPP2) were each tested as wall panels on the right-hand wall, covering an area of 25 m^2, as highlighted in Figure 24. The comparison of alpha values before and after the treatment revealed the proposed material’s impact on the acoustic performance within the room.

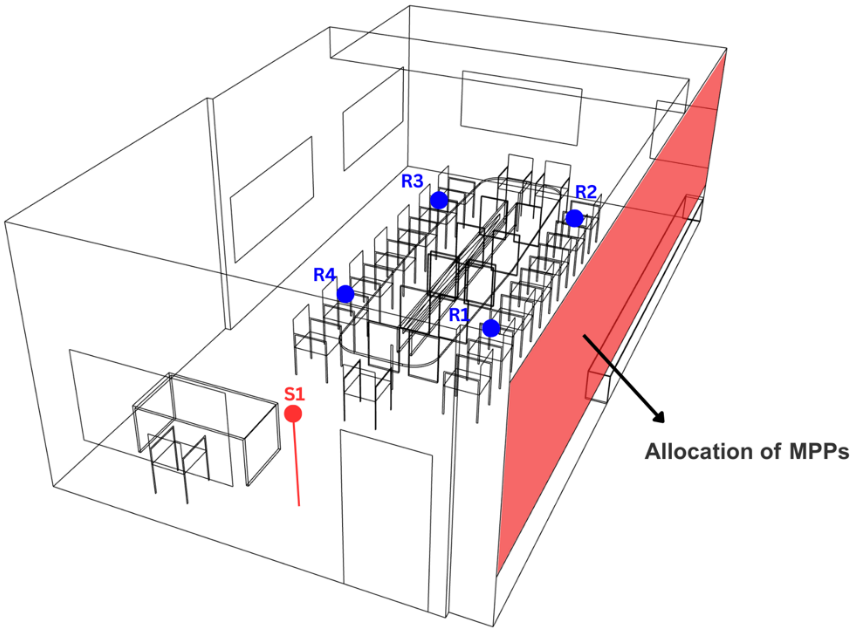

Figure 24. Position of the source and receivers with MPP allocation in the simulation

Table 5. Absorption coefficient of surfaces and materials in the room in 1/1 octave bands

Surfaces	**Materials**	**125 Hz**	**250 Hz**	**500 Hz**	**1000 Hz**	**2000 Hz**
Floor	Wood parquet	0.04	0.04	0.07	0.06	0.06
Wall	Painted wall	0.1	0.05	0.06	0.07	0.09
Ceiling	Painted wall	0.1	0.05	0.06	0.07	0.09
Windows	Ordinary glass windows	0.35	0.25	0.18	0.12	0.07
Door	Wooden door	0.14	0.1	0.06	0.08	0.1
Furniture	Fabric-covered Chairs	0.15	0.19	0.22	0.39	0.38
	Wooden desks	0.14	0.07	0.21	0.25	0.15
	Whiteboard	0.04	0.04	0.01	0.004	0.003
	Pinboard	0.1	0.2	0.35	0.3	0.25

CHAPTER IV

RESULTS

4.1. Impedance Tube Measurement Results

According to the measurement reports provided by BLX Acoustics Research Lab, Izmir, Türkiye, utilizing the transfer function method between the microphones, frequency-dependent sound absorption coefficient graphs were obtained to be analyzed in this section and in Section 5 for further discussion. PLA MPP (MPP1) and PET MPP (MPP2) are composed of four inhomogeneous sections, with each having different perforations and back cavity depths. The data yields unique peaks and dips in the plot, characteristic of each section. This means that each section is intrinsically effective at different frequency ranges, and when combined, they provide an absorption performance in wider frequency ranges. Further, each material exhibits its maximum absorption coefficient at its respective resonant frequency. To improve data consistency across five samples for each material type, mean α values were analyzed.

Impedance tube measurements according to the standard (ISO 10534-2:2023) demonstrated that MPP1 achieved a peak α value of 0.92 at 630 Hz (Figure 25). Starting from 200 Hz, MPP1 performed exponential growth in α until 630 Hz and gradually dropped below α values of 0.5 at 1600 Hz. Upon first observations, the findings showed satisfactory alignment with previous literature discussing the performance of MPPs made of PLA and its composites (Chin et al., 2018; Sekar et al., 2021a; Sailesh et al., 2021; Chin Vui et al., 2022; Rezaieyan et al., 2024). Across

1/3 octave bands, in the range of 400-1250 Hz, the samples yielded α values higher than 0.5. Considering the discrepancy in the first growth, the reported results explain that the reliability of the impedance tube method is negligible at frequencies below 250 Hz. The first peak at 500 Hz is explained by the effect of MPP1-a, with the lowest perforation ratio and largest back cavity among the sections, resulting in an α value of 0.86. The maximum absorption is achieved at 630 Hz (α = 0.92, SD = 0.06) peak, which is caused by MPP1-b, with a slightly smaller hole diameter and a 60 mm back cavity. The next peak at 1000 Hz (α = 0.89, SD = 0.03) is reached with MPP1-c. Then, the plot is dropped to an α value of 0.43 (SD = 0.06) at 1600 Hz, which is attributed to MPP1-d with the largest hole diameter (*d* = 2 mm) and the smallest back cavity of 20 mm. This section was aimed at improving the absorption at higher frequencies.

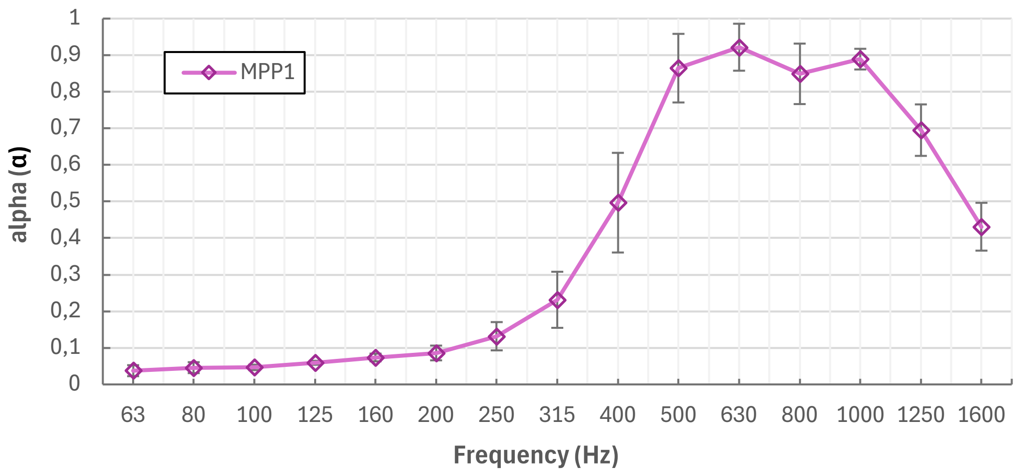

Figure 25. The absorption coefficients (α) of MPP1 at 1/3 octave bands

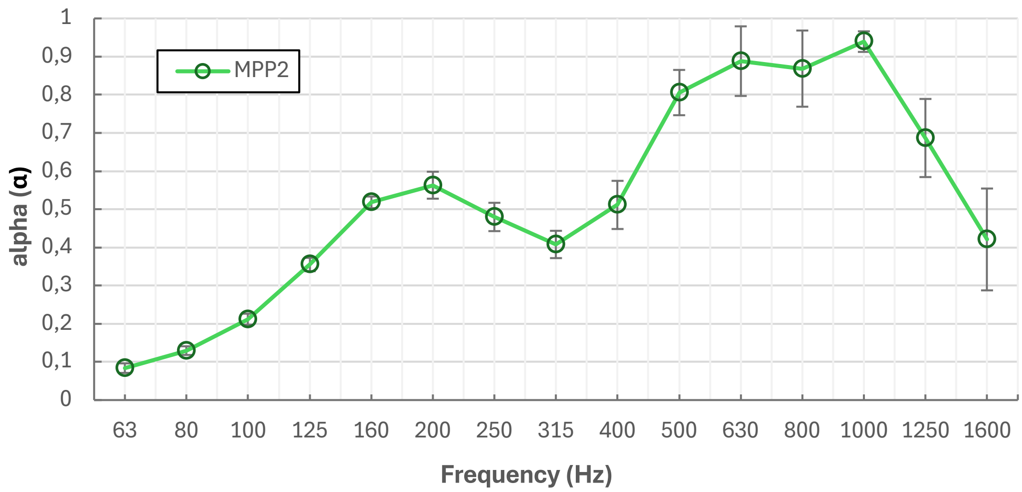

Figure 26. The absorption coefficients (α) of MPP2 at 1/3 octave bands

On the other hand, MPP2 demonstrated a twin-peak behavior (Figure 26). A better absorption performance is achieved in lower frequencies, particularly in the range of 125-400 Hz. MPP2-a shaped the first peak in the plot at 200 Hz (α = 0.56, SD = 0.03), which is achieved earlier than MPP1-a, but with 41% lower absorption. Unlike the exponential growth observed in MPP1, a valley-like behavior is demonstrated between 200-500 Hz. The inhomogeneous arrangement supported this mechanism to achieve absorption in a broader bandwidth, especially in lower frequencies.

At 400 Hz, the second peak is initiated, and an increase in α values is attributed to MPP2-b until 630 Hz (α = 0.89, SD = 0.09). A similar absorption ratio is attained until 1000 Hz, where the maximum absorption is obtained (α = 0.94, SD = 0.03) through the influence of MPP2-c. Past 1000 Hz, α values dipped below 0.7 at mid to higher frequencies, which demonstrated the high-frequency performance of MPP2-d. Overall, MPP2 showed a different absorption behavior compared to PET and its plastic-based composites (Li et al., 2017; Iannace & Ciaburro, 2021; Caniato et al., 2021, 2022). Additionally, in lower frequencies (63-315 Hz), it performed better than the organic-based (PLA) MPP while retaining a similar absorption at mid to high frequencies.

4.2. In-situ Measurement Results

4.2.2. Reverberation Time (RT30)

Figure 27 shows the RT30 in-situ measurement and simulated results of the classroom in an unoccupied condition. Both measured and simulated values failed to comply with the recommendations provided by the standards related to classrooms and their volumes. Under unoccupied, furnished conditions, RT30 should not exceed 0.6s and not fall behind 1s in the frequency range of 500-1000 Hz for classrooms with a volume less than 250 m^3 (Daniels & Bodkin, 2015; Chiu et al., 2015). However, in the current conditions of the classroom average reverberation time in mid frequencies exceeds 1s.

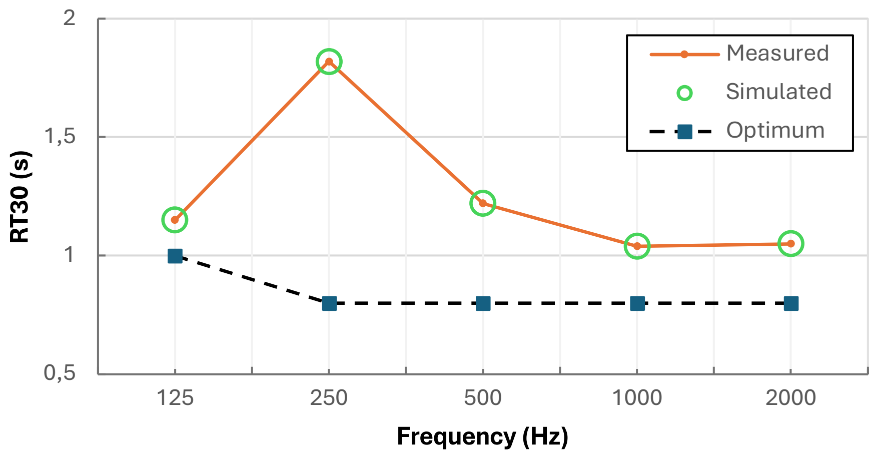

Figure 27. RT30 values for in-situ measured and simulated measurement results compared to the optimum value

Upon analyzing the plot, an increase in RT30 is displayed, particularly in the 125-500 Hz frequency range. With RT30 reaching 1.82s at 250 Hz, excessive reverberation is observed across all frequencies. This result highlighted the importance of sound absorption performance in low to mid frequencies, which is directly linked with speech-related sounds.

4.2.3. Speech Transmission Index (STI)

The measured Speech Transmission Index (STI) scores are generated by impulse response measurements taken in unoccupied and furnished room conditions, utilizing the DIRAC Acoustic Analyzer Software. The scores were adjusted by the software and averaged from STI $_{(male)}$ and STI $_{(female)}$. The scores were in the range of 0.52 and 0.53, which falls in the “fair” range in the speech intelligibility recommendations (Zhang et al., 2021).

4.3. Acoustic Simulation Measurement Results

4.3.1. Reverberation Time (RT30)

In acoustic simulation, ODEON Room Acoustics Software utilizes Geometrical Acoustics (GA), which requires absorption coefficients to be assigned to all surfaces.

Moreover, in a GA simulation, ray tracing and the image source method are used to simulate how sound travels across a space. Disregarding wave phenomena of sound, these methods simulate the travel of sound rays within a room while imitating their real-world behavior. To perform simulation measurements, the sound absorption coefficient results obtained from the impedance tube measurement were introduced into the software, as recommended by the literature (Cox & D'Antonio, 2017; Vorlander, 2020). The alpha values for each sample were processed into ODEON as hypothetical materials in 1/1 octave bands (Table 6). Similarly, virtual materials introduced for the room, in Section 3.3.2.2, are converted into the 1/1 octave band. Figure 28 displayed the impact of surfaces like glass windows, fabric-covered chairs, wooden desks and furniture, and the pinboard on the total absorption in the room. Materials with alpha values lower than 0.1 were not displayed in the plot as their impact on the absorption is very minimal. Then, the total sound absorption (∑A) was calculated according to Equation 2.1.

Table 6. Converted absorption coefficients in 1/1 octave bands

Frequency	125 Hz	250 Hz	500 Hz	1000 Hz	2000 Hz
MPP1	0.06	0.13	0.86	0.89	0.35
MPP2	0.35	0.48	0.8	0.94	0.34

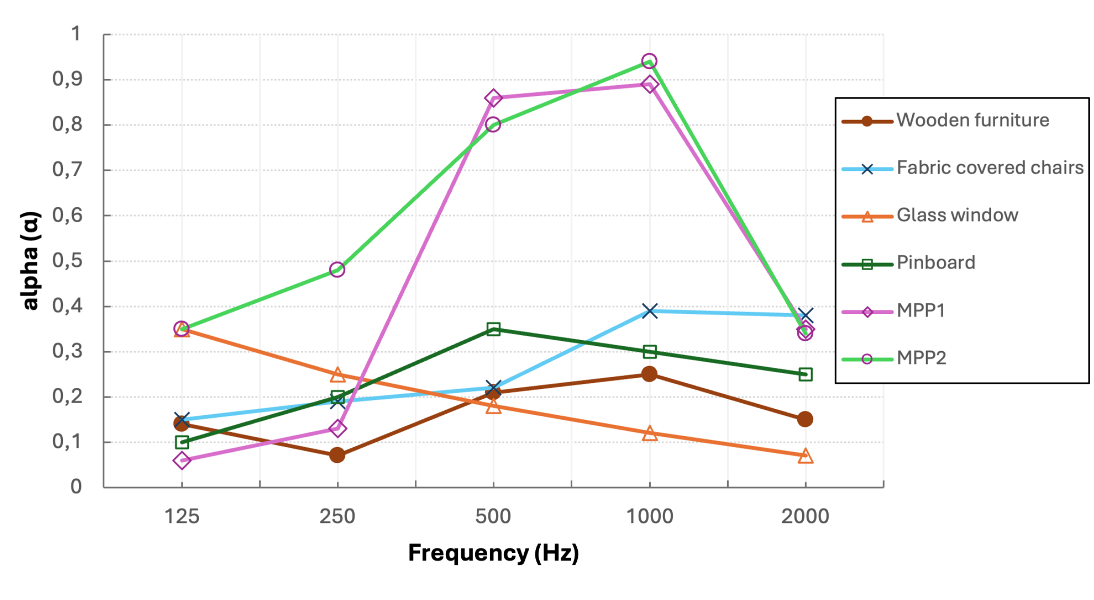

Figure 28. Alpha values of sound-absorbing materials within the room in 1/1 octave bands

The samples were integrated as an acoustic wall treatment with an area of 25 m^2, replacing the pinboard in the current condition. After implementing the treatment in the classroom, there is a visible change in RT30 values. Figure 29 highlights the change by comparing it to the untreated condition of the room. RT30 values with MPP1 were reduced by around 0.5s at all frequencies. The least impact in reducing the reverberant sound was observed at 250 Hz from 1.82s to 1.55s, and the most impact at 500 Hz from 1.22s to 0.7s. Overall, across 1/1 frequency bands, MPP1 underperformed in providing the necessary reduction in RT30, recommended by the optimum range. Conversely, treatment with MPP2 performed considerably better than MPP1 in reducing RT30. In lower frequencies, MPP2 outperformed MPP1 with around a 0.3-0.5s difference. Treatment with MPP2 reduced RT30 to its lowest point, 0.6s at 1000 Hz. Nonetheless, in the 500-2000 Hz frequency range, the samples worked similarly, averaging 0.73s in reverberant sound.

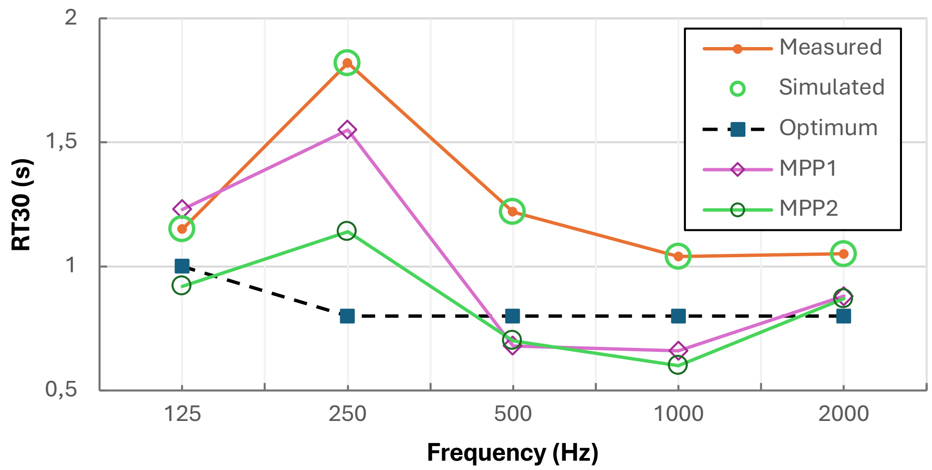

Figure 29. Measured and simulated RT30 results compared with MPP1 and MPP2 acoustic treatments

4.3.2. Speech Transmission Index (STI)

Additionally, speech intelligibility results were objectively measured using the Speech Transmission Index (STI) in the simulation. In this study, STI was measured according to the standard used for small to medium-sized speech purpose rooms, Noise Criteria 30 (NC30). The STI values for receivers in the room are in the “fair” range (Zhang et al., 2021), except for R4 at 0.6, which falls at the start of the “good” range. Similar to R4 scores, R1 values were improved by 0.5. The scores for R2 and R3 remained relatively unchanged between MPP1 and MPP2 treatments, considering their distant location from the sound source. Overall, the STI values range from a minimum score of 0.51 and a maximum score of 0.6, as listed in Table 7.

Table 7. STI values for each receiver in the room, compared with before and after treatments

STI	R1	R2	R3	R4
Before treatment	0.54	0.51	0.52	0.55
After MPP1 treatment	0.58	0.55	0.55	0.59
After MPP2 treatment	0.59	0.55	0.55	0.6

Additionally, it is important to highlight that the measurements conducted in ODEON were only performed with objective measurement methods. When assessing and evaluating the acoustics of an architectural space, both objective assessment and subjective evaluation methods should be emphasized, as the combination yields more accurate results. However, the objective assessment findings indicate that the implementation of sustainable alternatives to MPPs still significantly improves objective room acoustic parameters.

CHAPTER V

DISCUSSION

5.1. Micro-Perforated Panel (MPP) Performance

Utilizing both Equivalent Circuit Model (ECM) (Fasllija & Yilmazer, 2023; Fasllija, 2024) and Maa's Theory (1975; 1998), the micro-perforated panels (MPP) were designed. Addressing the Research Question, the results were found partially consistent with the question. Although there is a significant difference between the α values of MPP1 (PLA-MPP) and MPP2 (PET-MPP), mostly noticeable in the 63-315 Hz frequency bandwidth. MPP1's exponential α growth indicates that it performs worse in low frequencies, up to 315 Hz, where its performance matches that of MPP2. In contrast, the twin-peak behavior of MPP2 represents a superior absorption in low frequencies and a broader bandwidth than MPP1. This behavior also indicates that the inhomogeneous MPP mechanism works, which displays a similar plot to the findings from previous studies (Mosa et al., 2019; Laly et al., 2024) and specifically the study of Fasllija (2024). Furthermore, in the compared study, inhomogeneous acrylic MPP peaked at α = 0.91 at 500 Hz (Figure 30). MPP1 had peak absorption of α = 0.92 at 630 Hz, and MPP2 peaked with α = 0.94 at 1000 Hz. Overall, both MPP1 and MPP2 achieved greater α values; however, they underperformed at the 250-500 Hz frequency range compared to the acrylic MPP. To further extend their effective bandwidth, the back cavities can be installed with porous fibers, which improves their performance to a 2000-4000 Hz frequency range (Liu et al., 2017).

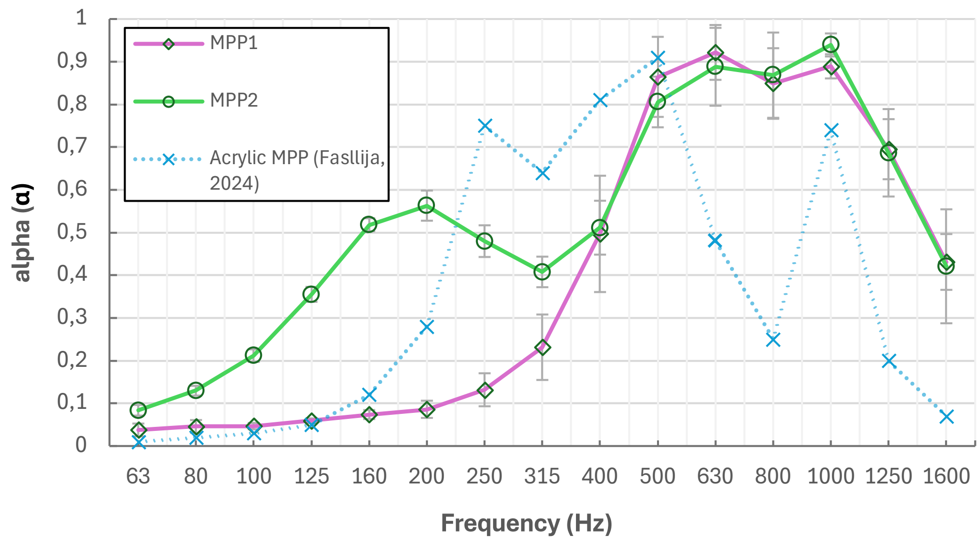

Figure 30. The absorption coefficients (α) of MPP1 and MPP2, at 1/3 octave bands, compared with the acrylic inhomogeneous MPP in a prior study by Fasllija (2024)

The findings also aligned with prior studies, which investigated the sound absorption coefficient (α) of pure PLA-MPP (MPP1) (Chin et al., 2018; Rezaieyan et al., 2024) and pure PET-MPP (MPP2) (Li et al., 2017). Exponential growth in α values of MPP1 after 400 Hz, followed by a reduction after 1000 Hz, showed similar prior studies (Sekar et al., 2021a; Sailesh et al., 2021; Chin Vui et al., 2022). However, MPP1 did not perform similarly to an inhomogeneous mechanism, lacking multiple resonant peaks (Fasllija & Yilmazer, 2023; Fasllija, 2024). This was interpreted by the researcher as a manufacturing limitation, 3D printing results being smoother for PET than for PLA, which may have resulted in irregular perforations, diminishing its low-frequency performance. Specifically, across samples, MPP1-a and MPP1-b performance may have been diminished. These configurations share the smallest perforation diameters (*d*) of 0.7 mm and 1 mm, which may have been printed irregularly by the printer. Additionally, the infill density could have affected the low-frequency performance. A prior study related to this issue (Sekar et al., 2022) stated that reducing the density also decreases the performance at low frequencies, as the sound wave propagation becomes harder inside the porous material. To compensate for the low-frequency performance, a thicker panel is required if the infill density remains low (Sekar et al., 2022). The discrepancy of MPP1 may have also originated from the sound leakage or porous holes of the material structure when inside the impedance tube. Any error may be possible during these experiments. Additionally, it is worth mentioning that relying solely on the 1/3 octave band results, eliminating other frequency bands, may have affected the accuracy of the results.

Conversely, the sustained absorption performance of MPP2 across low and mid frequencies yielded similar results to PET-based composites and inorganic polymers studied in previous literature (Li et al., 2017; Iannace & Ciaburro, 2021). This behavior may be attributed to a more porous structure caused by the curing process of the PET filament, as observed in the first manufactured samples. Moreover, MPP2 demonstrated the effect of its inhomogeneity, specifically caused by MPP2-a, MPP2-b, and MPP2-c. Compared to studies by Fasllija & Yilmazer (2023 and Fasllija (2024), MPP2 retained its resonant frequency after the second one.

Lastly, a review study by Zhang et al. (2023) stated that fibrous resonance mechanisms perform in a broader bandwidth in absorption than traditional fibrous sound-absorbing materials. In addition, a purer composite material, such as the study's MPPs, may have resulted in better sound absorption properties. According to the study by Shen et al. (2022), their outcome supported this, stating that composites with other materials are not essential if the appropriate geometric parameters and porosity are met. In this regard, the study contributed to the literature with a pure PLA and pure PET material comparison, as prior studies mostly focused on composites with other materials (Liu et al., 2016; Li et al., 2017; Chin et al., 2018; Sekar et al., 2021a; Iannace & Ciaburro, 2021; Caniato et al., 2021, 2022; Chin Vui et al., 2022; Beheshti et al., 2024).

5.2. Objective Acoustic Parameters Results

In the untreated classroom condition, RT30 exceeded recommended limits (Daniels & Bodkin, 2015; Chiu et al., 2015) compared to measured and simulated results. Previous studies (Choi, 2013; Cucharero et al., 2019; Labia et al., 2020) suggested optimal placement and configurations for absorbing materials on the ceiling, lateral walls, and upper wall parts. In the ODEON simulation, the samples were introduced as wall treatment panels, almost covering the right-hand wall of the classroom.

Application of the materials on a surface area of 25 m^2 significantly improved Reverberation Time (RT30) and Speech Transmission Index (STI) for all receivers within the room. However, it is important to highlight that the location and surface area of the material are dependent on factors such as room dimension, geometry and surface materials.

A prior study investigated in the same classroom (Yilmazer et al., 2024) confirmed the acoustically undertreated conditions. Their acoustic treatments with a composite PET-felt material reduced RT30 values below 1s, but it was not sufficient for the recommended levels. However, they improved STI scores from 0.48 to 0.62, which is satisfactory for classroom settings (Zhang et al., 2021). Relevant studies (Cingolani et al., 2021) investigated double-layer MPPs in historical classrooms related to acoustic simulations using Finite Difference Time Domain (FDTD). They improved RT30 and C50 results while comparing with Geometric Acoustics (GA) simulations, and FDTD provided more accurate results. Conversely, Pereira et al. (2021) investigated perforated panels and measured objective acoustic parameters entirely using a GA simulation. They obtained accurate results compared to real-world measurements. Compared to the treatment introduced in the study, MPP1 and MPP2 provided better improvement to RT30 at each frequency point.

MPP2 (PET-MPP) reduced RT30 from 1.82s to 1.55s at 250 Hz, compared to MPP1 (PLA-MPP)'s 1.67s. At 500 Hz, both MPPs achieved the recommended levels. Greater low-frequency effectiveness of MPP2 is particularly relevant, given that low-frequency reverberation has been stated as a limiting factor for speech intelligibility in classrooms (Sato & Bradley, 2008). Previous literature has recommended controlling early reflections, improving Clarity (C50), instead of reducing reverberation in low frequencies (Bradley et al., 2003). Additionally, an overall increase of STI values to 0.59-0.6 for both MPPs aligned with prior studies investigating the control of low-mid frequency reverberation (Sanavi et al., 2017; Campbell et al., 2019). The similar impact of both MPPs on improving STI reflects that STI is more sensitive to C50 low-to-mid frequency and the Signal-to-Noise Ratio (SNR) (Steeneken & Houtgast, 2002).

5.3. Contribution to Interior Applications

The geometric parameters of inhomogeneous MPPs were set constant; it can be interpreted that MPP1 and MPP2 provide a working alternative to inhomogeneous MPPs, which the literature did not have. In this regard, the outcomes and contributions of this study are found to be unique. Inhomogeneous MPPs (Mosa et al., 2019; Fasllija et al., 2021; Laly et al., 2024) and parallel-arranged MPPs (Fasllija, 2024) in prior studies showed that these mechanisms outperform conventional absorbers in terms of a broader bandwidth with more absorption efficiency, with less thickness, and without the need for fibrous materials in the back cavity. Additionally, the gap in the prior studies showed that comparisons between organic and inorganic-based inhomogeneous MPPs were nonexistent. In this regard, this study contributed to future studies on the comparison between organic and inorganic MPPs.

Apart from the engineering field, this study aims to enhance the acoustic conditions of interior spaces where speech is a crucial tool. Even though the arrangement and configurations of materials in the room acoustics field are an extensive research area on their own, the present study focuses on introducing the applicability of the investigated materials when implemented in interior settings. From a perspective concerning sustainability, both materials address the limitations of conventional absorbers, such as mineral wool, glass fiber, and foam, which pose challenges in recycling materials and threaten public health (Qiu, 2016; Arenas & Sakagami, 2020).

PLA's environmental benefits have been highlighted in previous studies (Sailesh et al., 2021; Sekar et al., 2021a). However, biodegradation tests in the literature (Sekar et al., 2021b) showed that PLA starts to lose 21% of its weight in four weeks, which may not be durable for architectural and interior use. However, PET with its plastic polymers provides a more reinforced structure (Li et al., 2017; Caniato et al., 2021, 2022). This study contributes to the literature by comparing organic PLA-MPP and inorganic recycled PET-MPP in identical geometrical configurations, supporting that both organic and inorganic MPPs are viable acoustic material options. Though in future studies, utilizing Life Cycle Assessments (LCA) of these materials could provide more accurate comparisons as to which materials hold better sustainable properties and better performance.

5.4. Limitations

The process of the study was challenged mainly by limitations related to the budget and time constraints. However, first, the MPP design process, specifically geometric parameters of MPPs, relied on a limited number of prior studies (Fasllija & Yilmazer, 2023; Fasllija, 2024) for comparability reasons, which may have eliminated the possibility of achieving the best absorption. The results in this study showed that PET-MPP provided promising results in terms of broadband absorption, while PLA-MPP needs further development in the design phase. It might be useful to utilize algorithm tools like MATLAB while considering all possible design options with a broader material range. The assumptions made with the hypothesis in Section 3.1.1. might have failed for this reason.

Moreover, most limitations were encountered in the manufacturing process of the study, namely, 3D printing. Fused Deposition Modelling (FDM), provided by 3D printing, allows for fast and clean manufacturing. However, 0.7 mm and 1 mm perforation diameters caused setbacks like unprinted holes and clogged nozzles. The printer provided by the Bilkent University Faculty of Fine Arts regularly undermined the manufacturing process. Some of the samples were decided to be printed at a manufacturer in Organize Sanayi Bölgesi (OSB), which changed the printer model, the adjusted printing settings, and the filament used before. Even then, some samples required manual drilling with the press machine and sanding the imperfections. Consequently, all the samples may not share the same surface characteristics, porosity, and absorption performance. The challenges mentioned above are explained in detail in section 3.2.2.

Additionally, the difference in low-frequency performance between MPP1 and MPP2 should be validated in a Reverberation Room (RR) measurement method (ISO 10534-1: 1996) with large-scale samples. Prior studies suggested (Fuchs & Zha, 1997; Fasllija, 2024) that only obtaining normal incidence absorption coefficients with impedance tube measurements (ISO 10534-2: 2023) may not be enough for accurate results, and random incidence may provide more realistic results as large-scale materials are measured. Due to time constraints and budget concerns, this phase of the study was eliminated.

Finally, to understand the room acoustic environment more accurately, subjective acoustic evaluations could have been implemented. The effect of perceived listening effort was not examined, as previous studies (Yilmazer et al., 2024; Fasllija, 2024) utilized this to evaluate the acoustic environment while integrating the impact of objective parameters. Even though the design and application of the proposed work may face practicality and reproducibility issues, the presented study offers an alternative solution to MPPs made of traditional materials while not compromising absorption performance.

CHAPTER VI

CONCLUSION

The objective of the study was to examine the acoustic performance of organic polylactic acid (PLA) based MPP and polyethylene terephthalate (PET) based MPP in a university classroom. The aim was to design a sustainable sound absorber that can achieve great low-frequency performance, while allowing architects to easily implement it into interior design. Following a comprehensive understanding of acoustic materials, design, and measurement trials were conducted to achieve a wideband sound absorber. The conclusions of the study are as follows:

6.1. Implications

The research contributes to the growing body of knowledge on sustainable acoustic materials by providing a direct, controlled comparison of two polymer-based MPPs under identical geometric and operational conditions. For practitioners in interior architecture and environmental design, the findings offer evidence-based guidance on integrating sustainable MPPs into classroom design without compromising acoustic performance. Moreover, the study underscores the feasibility of using additive manufacturing to produce precision-engineered acoustic panels, expanding design flexibility while minimizing waste.

From a sustainability perspective, both materials offer environmental advantages over conventional fibrous absorbers, which often present recycling challenges and potential health risks. PLA, as a biodegradable polymer, addresses end-of-life disposal concerns, while PET promotes circularity by utilizing post-consumer recycled content. The study's findings position these materials as practical and environmentally responsible alternatives for educational spaces.

6.2. Further Studies

Future research should address several limitations identified in this study. First, large-scale testing in a reverberation room (ISO 354:2003) is recommended to capture random-incidence absorption coefficients and improve the accuracy of low-frequency performance data. Second, a broader range of geometric parameter configurations should be explored, potentially optimized through computational modeling to maximize bandwidth and efficiency. Third, life cycle assessment (LCA) studies are needed to quantify the environmental impact of PLA and PET MPPs across their full production, use, and disposal phases.

Additionally, future investigations could incorporate subjective acoustic evaluation methods, such as perceived listening effort or affective soundscape assessments, to complement objective measurements and capture user-centered insights. In conclusion, this study demonstrates that biodegradable PLA and recycled PET MPPs are not only technically viable but also environmentally advantageous alternatives to conventional absorbers in educational spaces. Their distinct performance profiles allow for targeted acoustic design, while their sustainable attributes align with broader environmental objectives in architecture and interior design. By bridging acoustic performance and environmental responsibility, sustainable MPPs represent a promising alternative toward classrooms that are both good absorbers and sustainably designed.

BIBLIOGRAPHY

Adams, T. (2016). *Sound materials: a compendium of sound absorbing materials for architecture and design.* Frame Publishers.

Arenas, J. P., & Sakagami, K. (2020). Sustainable acoustic materials. *In Sustainability (Switzerland)* (Vol. 12, Issue 16). MDPI. https://doi.org/10.3390/su12166540

Arjunan, A., Baroutaji, A., & Latif, A. (2021). Acoustic behaviour of 3D printed titanium perforated panels. *Results in Engineering*, 11, 100252. https://doi.org/10.1016/j.rineng.2021.100252

Arvidsson, E., Nilsson, E., Bard-Hagberg, D., & Karlsson, O. J. I. (2021). Subjective Experience of Speech Depending on the Acoustic Treatment in an Ordinary Room. *Int. J. Environ. Res. Public Health 2021*, 18(23), 12274; https://doi.org/10.3390/ijerph182312274

Asdrubali, F., & Pispola, G. (2007). Properties of transparent sound-absorbing panels for use in noise barriers. The Journal of the Acoustical Society of America, 121(1), 214–221. https://doi.org/10.1121/1.2395916

Asdrubali, F., Schiavoni, S., & Horoshenkov, K. V. (2012). A Review of Sustainable Materials for Acoustic Applications. *Building Acoustics*, 19(4), 283–311. https://doi.org/10.1260/1351-010X.19.4.283

Aslan, R., & Turan, O. (2020). Gypsum-based sound absorber produced by 3D printing technology. *Applied Acoustics*, 161, 107162. https://doi.org/10.1016/j.apacoust.2019.107162

Astolfi, A., Bottalico, P., & Barbato, G. (2012). Subjective and objective speech intelligibility investigations in primary school classrooms. *The Journal of the Acoustical Society of America*, 131(1), 247–257. https://doi.org/10.1121/1.3662060

Barron, M. (2010). *Auditorium Acoustics and Architectural Design*. Spon Press

Beheshti, M. H., Khavanin, A., Jafarizaveh, M., & Tabrizi, A. (2024). A novel acoustic micro-perforated panel (MPP) based on sugarcane fibers and bagasse. *Journal of Materials Science: Materials in Engineering*, 19(1), 35. https://doi.org/10.1186/s40712-024-00173-9

Berardi, U., & Iannace, G. (2015). Acoustic characterization of natural fibers for sound absorption applications. *Building and Environment*, 94, 840–852. https://doi.org/10.1016/j.buildenv.2015.05.029

Bistafa, S. R., & Bradley, J. S. (2000). Predicting reverberation times in a simulated classroom. The Journal of the Acoustical Society of America, 108(4), 1721–1731. https://doi.org/10.1121/1.1310191

Bradley, J. S., Sato, H., & Picard, M. (2003). On the importance of early reflections for speech in rooms. The Journal of the Acoustical Society of America, 113(6), 3233–3244. https://doi.org/10.1121/1.1570439

Bradley, J. S., & Sato, H. (2008). The intelligibility of speech in elementary school classrooms. *The Journal of the Acoustical Society of America*, 123(4), 2078–2086. https://doi.org/10.1121/1.2839285

Broghany, M., & Basirjafari, S. (2022). Optimum Design of Multi-layered Micro-perforated Panel Sound Absorbers in Combination with Porous Materials in an Arbitrary Frequency Range. *International Journal of Engineering,* 35(5), 996–1005. https://doi.org/10.5829/IJE.2022.35.05B.15

Buratti, C., Belloni, E., Lascaro, E., Lopez, G. A., & Ricciardi, P. (2016). Sustainable Panels with Recycled Materials for Building Applications: Environmental and Acoustic Characterization. *Energy Procedia*, 101, 972–979. https://doi.org/10.1016/j.egypro.2016.11.123

Campbell, C., Sallenhag, H., Nilsson, E., & Arvidsson, E. (2019). Optimising the acoustic design for multi-purpose rooms used for a variety of speech communication activities (pp. 5952-5959). *Universitätsbibliothek der RWTH Aachen*.

Caniato, M., Cozzarini, L., Schmid, C., & Gasparella, A. (2021). Acoustic and thermal characterization of a novel sustainable material incorporating recycled microplastic waste. *Sustainable Materials and Technologies*, 28, e00274. https://doi.org/10.1016/j.susmat.2021.e00274

Caniato, M., Cozzarini, L., Schmid, C., & Gasparella, A. (2022). A sustainable acoustic customization of open porous materials using recycled plastics. *Scientific Reports*, 12(1), 10955. https://doi.org/10.1038/s41598-022-14009-z

Carbajo, J., Nam, S.-H., & Fang, N. X. (2024). Fabrication of Micro-Perforated Panel (MPP) sound absorbers using Digital Light Processing (DLP) 3D printing technology. Applied Acoustics, 216, 109788. https://doi.org/10.1016/j.apacoust.2023.109788

Chin, D. D. V. S., Yahya, M. N. B., Che Din, N. B., & Ong, P. (2018). Acoustic properties of biodegradable composite micro-perforated panel (BC-MPP) made from kenaf fibre and polylactic acid (PLA). Applied Acoustics, 138, 179–187. https://doi.org/10.1016/j.apacoust.2018.04.009

Chin Vui Sheng, D. D., Yahya, M. N. B., & Che Din, N. B. (2022). Sound Absorption of Microperforated Panel Made from Coconut Fiber and Polylactic Acid Composite. *Journal of Natural Fibers*, 19(7), 2719–2729. https://doi.org/10.1080/15440478.2020.1821290

Chiu, S., Noble, D., & Valmont, E. (2015). *Acoustics in architectural fabric structures*. In Fabric Structures in Architecture (pp. 241–256). Elsevier. https://doi.org/10.1016/B978-1-78242-233-4.00009-7

Christensen, C. L. (2023). Industrial, Auditorium and Combined Editions: Version 18.0 User Manual. Odeon Room Acoustics Program. Odeon A/S.

Choi, Y.-J. (2013). Effects of periodic type diffusers on classroom acoustics. *Applied Acoustics*, 74(5), 694–707. https://doi.org/10.1016/j.apacoust.2012.11.010

Ciaburro, G., & Iannace, G. (2022). Membrane-type acoustic metamaterial using cork sheets and attached masses based on reused materials. *Applied Acoustics*, 189, 108605. https://doi.org/10.1016/j.apacoust.2021.108605

Cingolani, M., Fratoni, G., Barbaresi, L., D'Orazio, D., Hamilton, B., & Garai, M. (2021). A Trial Acoustic Improvement in a Lecture Hall with MPP Sound Absorbers and FDTD Acoustic Simulations. *Applied Sciences*, 11(6), 2445. https://doi.org/10.3390/app11062445

Cobo, P., & Montero De Espinosa, F. (2013). Proposal of cheap microperforated panel absorbers manufactured by infiltration. Applied Acoustics, 74(9), 1069–1075. https://doi.org/10.1016/j.apacoust.2013.03.003

Cobo, P., & Simón, F. (2019). Multiple-Layer Microperforated Panels as Sound Absorbers in Buildings: A Review. Buildings, 9(2), 53. https://doi.org/10.3390/buildings9020053

Cobo, P., De La Colina, C., Roibás-Millán, E., Chimeno, M., & Simón, F. (2019). A wideband triple-layer microperforated panel sound absorber. Composite Structures, 226, 111226. https://doi.org/10.1016/j.compstruct.2019.111226

Cobo, P. (2021). Modelling of Microperforated Panel Absorbers with Circular and Slit Hole Geometries. Acoustics, 3(4), 665–678. https://doi.org/10.3390/acoustics3040042

Cox, T. J., & D'Antonio, P. (2017). *Acoustic absorbers and diffusers : theory, design, and application* (3rd edition). Spon Press.

Cucharero, J., Hänninen, T., & Lokki, T. (2019). Influence of Sound-Absorbing Material Placement on Room Acoustical Parameters. *Acoustics*, 1(3), Article 3. https://doi.org/10.3390/acoustics1030038

Çevresel Gürültünün Değerlendirilmesi ve Yönetimi Yönetmeliği (2022). Retrieved November, 30, 2022, from URL: https://www.mevzuat.gov.tr/mevzuat?MevzuatNo=39864&MevzuatTur=7&MevzuatTertip=5

Daniels, R., & Bodkin. (2015). *Acoustic design of schools: performance standards. Building Bulletin 93*.

Egan, M. D. (2007). *Architectural Acoustics.* J. Ross Publishing.

Everest, F. A. (2001). *Master Handbook of Acoustics, Fourth Edition*. McGraw-Hill Education.

Fasllija, E., Yilmazer, S. and Yilmazer, C., (2021). "A theoretical approach on designing wideband acoustic absorbers", *In Proceedings of Euronoise 2021* (pp. 1313-1322), Madeira, Portugal.

Fasllija, E., & Yilmazer, S. (2023). Investigating the Potential of Transparent Parallel-Arranged Micro-Perforated Panels (MPPs) as Sound Absorbers in Classrooms. *International Journal of Environmental Research and Public Health*, 20(2), 1445. https://doi.org/10.3390/ijerph20021445

Fasllija, E. (2024). Developing Wideband Acoustic Absorbers in Interior Spaces: Modelling, Measurements and Application [Doctoral thesis]. Bilkent University.

Fratoni, G., D'Orazio, D., De Salvio, D., & Garai, M. (2019). Predicting Speech Intelligibility In University Classrooms Using Geometrical Acoustic Simulations. In Building Simulation Conference Proceedings (Vol. 16, pp. 4305-4312). *IBPSA: International Building Performance Simulation Association.* https://doi.org/10.26868/25222708.2019.211161

Fuchs, H. (2013). *Applied acoustics: Concepts, absorbers, and silencers for acoustical comfort and noise control: Alternative solutions - Innovative tools - Practical examples*. Springer-Verlag Berlin Heidelberg. https://doi.org/10.1007/978-3-642-29367-2

Fuchs, H. V., & Zha, X. (1997). Acrylic-glass sound absorbers in the plenum of the Deutscher Bundestag. *Applied Acoustics*, 51(2), 211–217. https://doi.org/10.1016/S0003-682X(96)00064-3

Fuchs, H. V., & Zha, X. (2006). Micro-perforated structures as sound absorbers–a review and outlook. *Acta Acoustica united with Acoustica*, 92(1), 139-146.

Fowler, M. (2017). Architectures of Sound: Acoustic Concepts and Parameters for Architectural Design. In *Architectures of Sound: Acoustic Concepts and Parameters for Architectural Design*. Birkhauser Verlag AG.

Garcia-Valles, M., Avila, G., Martinez, S., Terradas, R., & Nogués, J. M. (2008). Acoustic barriers obtained from industrial wastes. *Chemosphere*, 72(7), 1098–1102. https://doi.org/10.1016/j.chemosphere.2008.03.039

Gautam, C., Garg, N., Ashish, A., Kamesh, Saini, P. K., & Devi, A. (2023). Sound Absorption Characteristics of Natural Fiber-Based Composite Sandwich Acoustical Materials. *MAPAN*, 38(4), 939–957. https://doi.org/10.1007/s12647-023-00672-8

González, A. E. (2019). How Do Acoustic Materials Work? IntechOpen. DOI: 10.5772/intechopen.82380

Herrin, D. W., Liu, W., Hua, X., & Liu, J. (2017). A Guide to the Application of Microperforated Panel Absorbers. *Sound and Vibration,* 51*,* 12-18.

Homkhiew, C., Srivabut, C., Boonchouytan, W., & Rawangwong, S. (2024). Sandwich composites from recycled plastic reinforced with krajood (Lepironia articulata) fiber for building applications. *Iranian Polymer Journal*. https://doi.org/10.1007/s13726-024-01292-y

Houtgast, T., Steeneken, H.J.M. (1973). The modulation transfer function in room acoustics as a predictor of speech intelligibility. *Acustica* 28(1973) 66-73.

Iannace, G., Trematerra, A., & Trematerra, P. (2013). Acoustic correction using green material in classrooms located in historical buildings. *Acoustics Australia*, 41(3), 213-218.

Iannace, G., & Ciaburro, G. (2021). Modelling sound absorption properties for recycled polyethylene terephthalate-based material using Gaussian regression. *Building Acoustics*, 28(2), 185–196. https://doi.org/10.1177/1351010X20933132

International Organization for Standardization. (1996). ISO 10534-1:1996 Acoustics — Determination of sound absorption coefficient and impedance in impedance tubes — Part 1: Method using standing wave ratio. https://www.iso.org/standard/18603.html

International Organization for Standardization. (2023). ISO 10534-2:2023 Acoustics — Determination of sound absorption coefficient and impedance in impedance tubes — Part 2: Transfer-function method. https://www.iso.org/standard/81294.html

International Organization for Standardization. (2009). ISO 3382-1:2009 Acoustics — Measurement of room acoustic parameters — Part 1: Performance spaces. https://www.iso.org/standard/40979.html

International Organization for Standardization. (2008). ISO 3382-2:2008 Acoustics — Measurement of room acoustic parameters — Part 2: Reverberation time in ordinary rooms. https://www.iso.org/standard/36201.html

International Organization for Standardization. (2022). ISO 3382-3:2022 Acoustics — Measurement of room acoustic parameters — Part 3: Open plan offices

International Organization for Standardization. (2003). ISO 354:2003 Acoustics — Measurement of sound absorption in a reverberation room. https://www.iso.org/standard/34545.html

Kang, J., & Fuchs, H. V. (1999). PREDICTING THE ABSORPTION OF OPEN WEAVE TEXTILES AND MICRO-PERFORATED MEMBRANES BACKED BY AN AIR SPACE. *Journal of Sound and Vibration*, 220(5), 905–920. https://doi.org/10.1006/jsvi.1998.1977

Kang, J., & Brocklesby, M. W. (2005). Feasibility of applying micro-perforated absorbers in acoustic window systems. Applied Acoustics, 66(6), 669–689. https://doi.org/10.1016/j.apacoust.2004.06.011

Kazmer, D. (2017). *Three-Dimensional Printing of Plastics. In Applied Plastics Engineering Handbook* (Second Edition, pp. 617–634). William Andrew Applied Science Publishers.

Kuttruff, H. (1991). Ultrasonics: Fundamentals and applications. *Elsevier Applied Science*, London, 363-394.

Kuttruff, H. (2006). *Room acoustics* (4th edition). Taylor & Francis.

Kumar, S., & Lee, H. (2019). The Present and Future Role of Acoustic Metamaterials for Architectural and Urban Noise Mitigations. *Acoustics*, 1(3), 590–607. https://doi.org/10.3390/acoustics1030035

Labia, L., Shtrepi, L., & Astolfi, A. (2020). Improved Room Acoustics Quality in Meeting Rooms: Investigation on the Optimal Configurations of Sound-Absorptive and Sound-Diffusive Panels. *Acoustics*, 2(3), Article 3. https://doi.org/10.3390/acoustics2030025

Laly, Z., Mechefske, C., Ghinet, S., Kone, T. C., Atalla, N., & Ashrafi, B. (2024). Improvement of the sound absorption performance of sandwich panel using inhomogeneous micro-perforations. *The Journal of the Acoustical Society of America*, 155(3_Supplement), A58–A58. https://doi.org/10.1121/10.0026791

Li, Y., & Ren, S. (2010). Acoustic and Thermal Insulating Materials. *Building Decorative Materials*, 359-374. https://doi.org/10.1533/9780857092588.359

Li, G., Tang, X., Zhang, X., Qian, Y. J., & Kong, D. (2017). Investigation on the Acoustic Absorption of Flexible Micro-Perforated Panel with Ultra-Micro Perforations. *IOP Conference Series: Materials Science and Engineering*, 269, 012023. https://doi.org/10.1088/1757-899X/269/1/012023

Liu, Z., Zhan, J., Fard, M., & Davy, J. L. (2016). Acoustic properties of a porous polycarbonate material produced by additive manufacturing. Materials Letters, 181, 296–299. https://doi.org/10.1016/j.matlet.2016.06.045

Liu, Z., Zhan, J., Fard, M., & Davy, J. L. (2017). Acoustic measurement of a 3D printed micro-perforated panel combined with a porous material. Measurement, 104, 233–236. https://doi.org/10.1016/j.measurement.2017.03.032

Maa, D.-Y. (1998). Potential of microperforated panel absorber. *The Journal of the Acoustical Society of America*, *104*(5), 2861–2866. https://doi.org/10.1121/1.423870

Maa, D. (1975). Theory and design of microperforated panel sound-absorbing constructions. *Scient. Sin.*, *18*(1), 55–71.

Mogan, J., Harun, W. S. W., Kadirgama, K., Ramasamy, D., Foudzi, F. M., Sulong, A. B., Tarlochan, F., & Ahmad, F. (2023). Fused Deposition Modelling of Polymer Composite: A Progress. *Polymers*, 15(1), 28. https://doi.org/10.3390/polym15010028

Mosa, A. I., Putra, A., Ramlan, R., Prasetiyo, I., & Esraa, A.-A. (2019). Theoretical model of absorption coefficient of an inhomogeneous MPP absorber with multi-cavity depths. *Applied Acoustics*, 146, 409–419. https://doi.org/10.1016/j.apacoust.2018.11.002

Minelli, G., Puglisi, G. E., & Astolfi, A. (2022). Acoustical parameters for learning in classroom: A review. *Building and Environment*, 208, 108582. https://doi.org/10.1016/j.buildenv.2021.108582

Ngo, T. D., Kashani, A., Imbalzano, G., Nguyen, K. T. Q., & Hui, D. (2018). Additive manufacturing (3D printing): A review of materials, methods, applications and challenges. *Composites Part B: Engineering*, 143, 172–196. https://doi.org/10.1016/j.compositesb.2018.02.012

Nocke, C. (2019). 20 years of micro-perforated (transparent) sound absorbers. *Australian Acoustical Society AAS2019: Acoustics 2019 - Sound Decisions: Moving forward with Acoustics, Victoria, Australia.*

Padhye, R., & Nayak, R. (2016). Acoustic Textiles. Springer Singapore. https://doi.org/10.1007/978-981-10-1476-5

Patil, C., Ghorpade, R., & Askhedkar, R. (2024). Analysing the Impact of 3D-Printed Perforated Panels and Polyurethane Foam on Sound Absorption Coefficients. Modelling, 5(3), 969–989. https://doi.org/10.3390/modelling5030051

Peng, T., & Sun, W. (2017). Energy modelling for FDM 3D printing from a life cycle perspective. *International Journal of Manufacturing Research*, 12(1), 83. https://doi.org/10.1504/IJMR.2017.083651

Pereira, A., Gaspar, A., Godinho, L., Amado Mendes, P., Mateus, D., Carbajo, J., Ramis, J., & Poveda, P. (2021). On the Use of Perforated Sound Absorption Systems for Variable Acoustics Room Design. *Buildings*, 11(11), 543. https://doi.org/10.3390/buildings11110543

Qiu, X. (2016). Principles of Sound Absorbers. In *Acoustic Textiles* (pp. 43–72). https://doi.org/10.1007/978-981-10-1476-5_3

Qian, Y. J., Kong, D. Y., Liu, S. M., Sun, S. M., & Zhao, Z. (2013). Investigation on micro-perforated panel absorber with ultra-micro perforations. Applied Acoustics, 74(7), 931–935. https://doi.org/10.1016/j.apacoust.2013.01.009

Rezaieyan, E., Taban, E., Berardi, U., Mortazavi, S. B., Faridan, M., & Mahmoudi, E. (2024). Acoustic properties of natural fiber reinforced composite micro-perforated panel (NFRC-MPP) made from cork fiber and polylactic acid (PLA) using 3D printing. *Journal of Building Engineering*, 84, 108491. https://doi.org/10.1016/j.jobe.2024.108491

Prasetiyo, I., Sihar, I., & Sudarsono, A. S. (2021). Realization of a thin and broadband microperforated panel (MPP) sound absorber. Applied Acoustics, 183, 108295. https://doi.org/10.1016/j.apacoust.2021.108295

Ruiz, H., Cobo, P., & Jacobsen, F. (2011). Optimization of multiple-layer microperforated panels by simulated annealing. Applied Acoustics, 72(10), 772–776. https://doi.org/10.1016/j.apacoust.2011.04.010

Ruiz, H., Cobo, P., Dupont, T., Martin, B., & Leclaire, P. (2012). Acoustic properties of plates with unevenly distributed macroperforations backed by woven meshes. The Journal of the Acoustical Society of America, 132(5), 3138–3147. https://doi.org/10.1121/1.4754520

Sabine, W.C. (1923). The American Architect 1900, see also Collected Papers on Acoustics No. 1, *Harvard University Press, Cambridge.*

Sailesh, R., Yuvaraj, L., Pitchaimani, J., Doddamani, M., & Mailan Chinnapandi, L. B. (2021). Acoustic behaviour of 3D printed bio-degradable micro-perforated panels with varying perforation cross-sections. *Applied Acoustics*, *174*, 107769. https://doi.org/10.1016/j.apacoust.2020.107769

Sakagami, K., Morimoto, M., Yairi, M., & Minemura, A. (2008). A pilot study on improving the absorptivity of a thick microperforated panel absorber. Applied Acoustics, 69(2), 179–182. https://doi.org/10.1016/j.apacoust.2006.09.008

Sakagami, K., Nagayama, Y., Morimoto, M., & Yairi, M. (2009). Pilot study on wideband sound absorber obtained by combination of two different microperforated panel (MPP) absorbers. Acoustical Science and Technology, 30(2), 154–156. https://doi.org/10.1250/ast.30.154

Sakagami, K., Kusaka, M., Okuzono, T., Kido, S., & Yamaguchi, D. (2021). Application of transparent microperforated panels to acrylic partitions for desktop use: A case study by prototyping. UCL Open Environment, 2. https://doi.org/10.14324/111.444/ucloe.000021

Salandin, A., Quintana-Gallardo, A., Gómez-Lozano, V., & Guillén-Guillamón, I. (2022). The First 3D-Printed Building in Spain: A Study on Its Acoustic, Thermal and Environmental Performance. *Sustainability*, 14(20), 13204. https://doi.org/10.3390/su142013204

Sanavi, A., Schäffer, B., Heutschi, K., & Eggenschwiler, K. (2017). On the Effect of an Acoustic Diffuser in Comparison with an Absorber on the Subjectively Perceived Quality of Speech in a Meeting Room. Acta Acustica United with Acustica, 103(6), 1037–1049. https://doi.org/10.3813/AAA.919133

Sato, H., & Bradley, J. S. (2008). Evaluation of acoustical conditions for speech communication in working elementary school classrooms. *The Journal of the Acoustical Society of America*, 123(4), 2064–2077. https://doi.org/10.1121/1.2839283

Sekar, V., Eh Noum, S. Y., Sivanesan, S., Putra, A., Kassim, D. H., Wong, Y. S., & Chin, K. C. (2021a). Effect of Perforation Volume on Acoustic Absorption of the 3D Printed Micro-Perforated Panels made of Polylactic Acid reinforced with Wood Fibers. *Journal of Physics: Conference Series*, 2120(1), 012039. https://doi.org/10.1088/1742-6596/2120/1/012039

Sekar, V., Zarrouq, M., & Namasivayam, S. N. (2021b). Development and Characterization of Oil Palm Empty Fruit Bunch Fibre Reinforced Polylactic Acid Filaments for Fused Deposition Modeling. *Journal of Mechanical Engineering*, 18(1), 89–107. https://doi.org/10.24191/jmeche.v18i1.15167

Sekar, V., Eh Noum, S. Y., Sivanesan, S., Putra, A., Chin Vui Sheng, D. D., & Kassim, D. H. (2022). Effect of Thickness and Infill Density on Acoustic Performance of 3D Printed Panels made of Natural Fiber Reinforced Composites. Journal of Natural Fibers, 19(13), 7132–7140. https://doi.org/10.1080/15440478.2021.1944426

Selim, A. M., & Saeed, D. M. (2022). Enhancing the classroom acoustic environment in Badr University, Egypt: A case study. Building Acoustics, 29(4), 577–596. https://doi.org/10.1177/1351010X221119381

Shen, J., Lee, H. P., & Yan, X. (2022). Sound absorption performance and mechanism of flexible PVA microperforated membrane. *Applied Acoustics*, 185, 108420. https://doi.org/10.1016/j.apacoust.2021.108420

Sheng, S., & Mo, F. (2010). Study on wooden micro-perforated panel and its application. Proceedings of 20th International Congress on Acoustics, ICA 2010, Sydney, Australia.

Shield, B. M., & Dockrell, J. E. (2008). The effects of environmental and classroom noise on the academic attainments of primary school children. *The Journal of the Acoustical Society of America*, 123(1), 133–144. https://doi.org/10.1121/1.2812596

Steeneken, H. J. M., & Houtgast, T. (2002). Validation of the revised STIr method. Speech Communication, 38(3–4), 413–425. https://doi.org/10.1016/S0167-6393(02)00010-9

Stoof, D., Pickering, K., & Zhang, Y. (2017). Fused Deposition Modelling of Natural Fibre/Polylactic Acid Composites. *Journal of Composites Science*, 1(1), 8. https://doi.org/10.3390/jcs1010008

Xu, X., Wang, H., Sun, Y., Han, J., & Huang, R. (2018). Sound absorbing properties of perforated composite panels of recycled rubber, fiberboard sawdust, and high density polyethylene. Journal of Cleaner Production, 187, 215–221. https://doi.org/10.1016/j.jclepro.2018.03.174

Vorländer, M. (2020). Auralization: Fundamentals of Acoustics, Modelling, Simulation, Algorithms and Acoustic Virtual Reality. Springer International Publishing. https://doi.org/10.1007/978-3-030-51202-6

Yang, W., Bai, X., Zhu, W., Kiran, R., An, J., Chua, C. K., & Zhou, K. (2020). 3D Printing of Polymeric Multi-Layer Micro-Perforated Panels for Tunable Wideband Sound Absorption. *Polymers*, 12(2), 360. https://doi.org/10.3390/polym12020360

Yilmazer, S., Keseci, T., & Fasllija, E. (2024). Objective and subjective assessment of PET felt recycled panels as an acoustic treatment in the meeting rooms. *INTER-NOISE and NOISE-CON Congress and Conference Proceedings. INTER-NOISE24*, *Nantes, France*. 485-494(10).

Zhang, D., Tenpierik, M., & Bluyssen, P. M. (2021). Individual control as a new way to improve classroom acoustics: A simulation-based study. *Applied Acoustics*, 179, 108066. https://doi.org/10.1016/j.apacoust.2021.108066

Zhang, C., Li, H., Gong, J., Chen, J., Li, Z., Li, Q., Cheng, M., Li, X., & Zhang, J. (2023). The review of fiber-based sound-absorbing structures. *Textile Research Journal*, 93(1–2), 434–449. https://doi.org/10.1177/00405175221084736